



AMERICAN UNIVERSITY OF BEIRUT

INTEGRATION OF MICROELECTROLYSIS CELL (MEC)  
WITH ANAEROBIC FLUIDIZED MEMBRANE  
BIOREACTOR (ANFMBR) TECHNOLOGY FOR  
WASTEWATER TREATMENT AND REUSE

by  
OLGA SAMIR EL KIK

A thesis  
submitted in partial fulfillment of the requirements  
for the degree of Master of Engineering  
to the Department of Civil and Environmental Engineering  
of the Faculty of Engineering and Architecture  
at the American University of Beirut

Beirut, Lebanon  
May 2020

AMERICAN UNIVERSITY OF BEIRUT

INTEGRATION OF MICROELECTROLYSIS CELL (MEC)  
WITH ANAEROBIC FLUIDIZED MEMBRANE  
BIOREACTOR (ANFMBR) TECHNOLOGY FOR  
WASTEWATER TREATMENT AND REUSE

by

OLGA SAMIR EL KIK

Approved by:

---

Dr. Mutasem El- Fadel, Professor  
Department of Civil and Environmental Engineering, AUB

Advisor

---

Dr. Pascal E. Saikaly, Associate Professor  
Biological and Environmental Science and  
Engineering Division, KAUST

Co-Adviser

---

Dr. Ibrahim Alameddine, Assistant Professor  
Department of Civil and Environmental Engineering, AUB

Member of Committee

Date of thesis defense: February 13, 2020

AMERICAN UNIVERSITY OF BEIRUT

INTEGRATION OF MICROELECTROLYSIS CELL (MEC) WITH  
ANAEROBIC FLUIDIZED MEMBRANE BIOREACTOR (ANFMBR)  
TECHNOLOGY FOR WASTEWATER TREATMENT AND REUSE

by

OLGA SAMIR EL KIK

Approved by:



---

Dr. Mutasem El- Fadel, Professor  
Department of Civil and Environmental Engineering, AUB

Advisor

---

Dr. Pascal E. Saikaly, Associate Professor  
Biological and Environmental Science and  
Engineering Division, KAUST



Co-Advisor

---

Dr. Ibrahim Alameddine, Assistant Professor  
Department of Civil and Environmental Engineering, AUB

Member of Committee



Date of thesis defense: February 13, 2020

# AMERICAN UNIVERSITY OF BEIRUT

## THESIS, DISSERTATION, PROJECT RELEASE FORM

Student Name: El Kik Olga Samir  
Last First Middle

Master's Thesis       Master's Project       Doctoral Dissertation

I authorize the American University of Beirut to: (a) reproduce hard or electronic copies of my thesis, dissertation, or project; (b) include such copies in the archives and digital repositories of the University; and (c) make freely available such copies to third parties for research or educational purposes.

I authorize the American University of Beirut, to: (a) reproduce hard or electronic copies of it; (b) include such copies in the archives and digital repositories of the University; and (c) make freely available such copies to third parties for research or educational purposes

after:

**One ---year from the date of submission of my thesis, dissertation, or project.**

**Two --- years from the date of submission of my thesis, dissertation, or project.**

**Three ~~X~~ years from the date of submission of my thesis, dissertation, or project.**



20/05/2020

Signature

Date



# AMERICAN UNIVERSITY OF BEIRUT

## THESIS, DISSERTATION, PROJECT RELEASE FORM

Student Name: El Kik Olga Samir  
Last First Middle

Master's Thesis       Master's Project       Doctoral Dissertation

I authorize the American University of Beirut to: (a) reproduce hard or electronic copies of my thesis, dissertation, or project; (b) include such copies in the archives and digital repositories of the University; and (c) make freely available such copies to third parties for research or educational purposes.

I authorize the American University of Beirut, to: (a) reproduce hard or electronic copies of it; (b) include such copies in the archives and digital repositories of the University; and (c) make freely available such copies to third parties for research or educational purposes

after:

**One ---year from the date of submission of my thesis, dissertation, or project.**

**Two --- years from the date of submission of my thesis, dissertation, or project.**

**Three ---- years from the date of submission of my thesis, dissertation, or project.**

---

Signature

Date

## ACKNOWLEDGMENTS

I would like to thank my advisor Prof. Mutasem El-Fadel, for his continuous support, and patient guidance. It was a great honor to have him as my advisor throughout my master's program.

I am equally thankful to my thesis committee members, Dr. Pascal Saikaly and Dr. Ibrahim Alameddine for their constructive criticism, expertise, time and effort in improving this work.

I would like to express my deepest appreciation to Dr. Krishna Katuri for his help in the start-up phase and his assistance and incessant advice during the experimental process.

I would like also to thank Mr. Helmi El-Khatib, Ms. Dima El Hassaniah, Ms. Christiane Chedid, Mr. Ramez Zayyat, Mr. Joseph Dawud, Ms. Zakeeya Dib and Ms. Rania Shatila for their support and generous assistance.

I want to thank deeply my dear friend and amazing experimental and writing partner Ms. Lea Issa with whom I shared all the good and bad days of the experiment.

Special thanks go to my beloved family and husband for their endless love and enormous support and encouragement throughout these academic years.

Lastly, I would like to thank Dar Al-Handasah (Shair & Partners) for their support to the graduate programs in Engineering at the American University of Beirut. Special thanks are extended to the Center Competitive Funding Program (FCC/1/1971-05-01) from King Abdullah University of Science and Technology (KAUST) for their contribution to the experimental program.



## AN ABSTRACT OF THE THESIS OF

Olga Samir El Kik for Master of Engineering  
Major: Environmental and Water Resources Engineering

Title: Integration of Microelectrolysis cell (MEC) with Anaerobic Fluidized Membrane Bioreactor (AnFMBR) for wastewater treatment and reuse

Anaerobic Membrane Bioreactors (AnMBRs) combine the advantages of anaerobic processes and MBR technology to increase effluent quality and recover energy. However, these systems are associated with several operational challenges such as membrane fouling and loss of dissolved methane which increase operation and energy expenses. In this study, a new system configuration was developed that combines an anaerobic fluidized membrane bioreactor (AnFMBR) with a Microbial Electrolysis Cell (MEC) and tested for the treatment of synthetic wastewater. The effects of electrochemical reactions in the AnFMBR-MEC were examined in terms of Chemical Oxygen Demand (COD) removal, biogas generation, fouling potential, and microbial community characteristics. The startup of the AnFMBR-MEC system was 25 days faster than the AnFMBR alone. While both reactors exhibited a high COD removal (~90%), the new AnFMBR-MEC system enhanced the average methane yield by 56%. In addition, the new system reduced membrane fouling with a maximum transmembrane pressure value nearly 6.5 folds lower than that exhibited by the AnFMBR. Similar bacterial community existed in both reactors but with different abundance and localization. In the AnFMBR-MEC, Direct Interspecies Electron Transfer was possibly the dominant route for acetate consumption due to the abundance of *Geobacter* and *Methanosarcina* on granular activated carbon and in suspension. Taken together, the new AnFMBR-MEC system provides a promising technology for recovery of resources (reclaimed water for non-potable reuse and energy) from wastewater.

# CONTENTS

ACKNOWLEDGMENTS.....	V
ABSTRACT .....	VI
LIST OF ILLUSTRATIONS .....	IX
LIST OF TABLES .....	X
LIST OF ABBREVIATIONS .....	XI

Chapter

I.INTRODUCTION .....	1
II.MATERIALS AND METHODS .....	5
A. Reactor configuration.....	5
B. Reactor Start-up and Operation .....	7
C. Analysis.....	7
1. COD and biogas analysis .....	7
2. Scanning Electron Microscopy (SEM) .....	8
3. DNA extraction, Library preparation, sequence and analysis .....	9
4. Voltage and transmembrane pressure (TMP) measurements .....	10
5. Energy Requirements and Production .....	11
III.RESULTS AND DISCUSSION .....	13
A. Start-up phase.....	13
B. COD, biogas and electrochemical performance during operation phase.....	14

C. Fouling during operation phase ..... 19  
D. Energy balance..... 22  
E. Microbial Community..... 23

IV.CONCLUSION .....27

REFERENCES .....28

Appendices

APPENDIX A.....35

# ILLUSTRATIONS

Figure	page
1: AnFMBR MEC and AnFMBR Setup .....	6
2: Detailed reactor configuration of AnFMBR-MEC .....	6
3: COD removal (weekly average) in both reactors during operation phase .....	17
4: Methane yields (average weekly) for both reactors during operation phase. ....	18
5: Electrochemical performance of the AnFMBR-MEC during operation phase.....	19
6: Transmembrane pressure (TMP) values during operation phase.....	21
7: The 40 most abundant genera (or lowest taxonomic classification level possible with f representing family level and o representing order level) in the AnFMBR and AnFMBR-MEC during the operation phase. ....	24
8: Virgin vs. biofouled HFM surface and biofilm covered anode and cathode. ....	26
9: Experimental set-up during installation.....	39
10: Purging the synthetic feed tank with nitrogen (GC Unit on the right).....	39
11: Power supply unit .....	40
12: Experimental set-up during operation.....	40

# TABLES

Table	page
1: Synthetic wastewater composition (Wang et al., 2013, Katuri et al., 2010).....	8
2: Performance of the AnFMBR-MEC.....	18
3: Comparison between AnFMBR and AnFMBR-MEC during stable performance.....	20
4: Acetate and COD removal data.....	35
5: Energy parameters during operation.....	36

## ABBREVIATIONS

AnEMBR	Anaerobic Electrochemical Membrane Bioreactor
AnFMBR	Anaerobic Fluidized Membrane Bioreactor
AnMBR	Anaerobic Membrane Bioreactor
AnFMBR-MEC	Anaerobic Membrane Bioreactor coupled with Micro Electrolysis Cell
CAS	Conventional Activated Sludge
CE	Coulombic Efficiency
CEM	Cation Exchange Membrane
CH <sub>4</sub>	Methane
CO <sub>2</sub>	Carbon Dioxide
COD	Chemical Oxygen Demand
CSTR	Completely Stirred Tank Reactor
DIET	Direct Interspecies Electron Transfer
DNA	Deoxyribonucleic Acid
EAB	Electrochemically Active Bacteria
GAC	Granular Activated Carbon
GC	Gas Chromatographer
H <sub>2</sub>	Hydrogen
H <sub>2</sub> O	Water
HER	Hydrogen Evolution Reaction
HFM	Hollow Fiber Membrane
HRT	Hydraulic Retention Time
LMH	L/m <sup>2</sup> /h
MBR	Membrane Bioreactor (aerobic)
MEC	Microbial Electrolysis Cell
MFC	Microbial Fuel Cell

MLSS	Mixed Liquor Suspended Solids
N <sub>2</sub>	Nitrogen
OLR	Organic Loading Rate
SEM	Scanning Electron Microscope
SRB	Sulfate-Reducing Bacteria
SRT	Solid Retention Time
TMP	Transmembrane Pressure
VFA	Volatile Fatty Acids

# CHAPTER I

## INTRODUCTION

Population growth and development are continuously stressing natural resources particularly water and energy. In this context, wastewater treatment offer a promising source of clean water for reuse (Pechan et al., 2013). Membrane Bioreactors (MBRs) have attracted interests during the last two decades for wastewater treatment and reuse (Lin et al., 2013), combining membrane separation with biological treatment of wastewater to generate effluent water quality suitable for reuse (Ahmed and Lan, 2012). The MBR based on activated sludge process offers several advantages including higher removal performance, compactness and smaller footprint, and ease in adaptation to existing works (Lin et al., 2013, Sutherland, 2010, Melin et al., 2006, Tchobanoglous et al., 2003). However, it is an energy intensive (1–2 kWh/m<sup>3</sup>) technology where a large fraction of this energy is used for aeration, filtration process, and scouring of the membranes to minimize fouling (Werner et al., 2016). Recently, there has been an increasing interest in anaerobic MBR (AnMBR) for wastewater treatment and reuse due to their lower energy demand (no aeration), energy recovery as methane due to the activity of methanogenic archaea (Farhadian et al., 2007), high COD removal and high ammonia tolerance (Krzeminski et al., 2017, Hashisho and El-Fadel, 2016, Luo et al., 2015, Trzcinski and Stuckey, 2016), as well as sludge reduction and stabilization (Khan et al., 2016).

Similar to aerobic MBRs, fouling also occurs in AnMBR and is considered one of the major limitation for its application because of the higher biomass concentration in long-



term operations (Hashisho and El-Fadel, 2016). In general, biogas sparging has been widely used to control fouling in AnMBR. However, this method has high energy requirements ranging from 0.7 to 3.4 kWh/m<sup>3</sup> (Aslam et al., 2018). As such, alternative methods with low electrical energy requirement (0.1 kWh/m<sup>3</sup>) have been developed to control fouling such as the addition of Granular Activated Carbon (GAC) with biogas sparging/fluidization (Shin and Bae, 2018, Kim et al., 2011). In addition to being energy efficient, GAC fluidization provides mechanical cleaning of the membrane and a high surface area for biomass growth (Aslam and Kim, 2019, Yoo et al., 2012, Kim et al., 2011).

Recently, more efforts are directed towards other anaerobic processes that utilize the potential of electrochemically active bacteria (EAB), also known as electricigens, to oxidize organic carbon, while simultaneously transferring the generated electrons to an anode in a microbial electrochemical system. The electrons and protons generated by EAB are then transferred to the cathode through an external circuit and electrolyte, respectively, where they are reduced to water in the presence of oxygen (in microbial fuel cell, MFC) or hydrogen with the use of an external voltage under anaerobic conditions (in microbial electrolysis cell, MEC) (Katuri et al., 2018, Logan and Rabaey, 2012, Liu et al., 2010).

While MFC or MEC offer the opportunity to offset energy consumption for wastewater treatment, they cannot be used as a standalone technology for generating effluent water quality suitable for reuse, i.e., they need to be coupled with membrane filtration processes (Katuri et al., 2014). For example, MFCs were combined with a flat-sheet ultrafiltration membrane biocathode (Cao et al., 2017, Liu et al., 2014, Malaeb et al., 2013, Xu et al., 2015). In other studies, the membrane filtration unit was placed between

the anode and cathode of MFCs (Gajaraj and Hu, 2014, Li et al., 2014, Liu et al., 2013, Tian et al., 2014, Wang et al., 2018, Wang et al., 2011, Wang et al., 2013, Wang et al., 2012), or outside the MFC (Borea et al., 2017, Wang et al., 2016, Ren et al., 2014, Su et al., 2013). As for MECs, only few studies coupled MEC with membrane filtration, in what is referred to as anaerobic electrochemical membrane bioreactor (AnEMBR) (Sapireddy et al., 2019, Ding et al., 2018, Werner et al., 2016, Katuri et al., 2014). For example, electrocatalytic and porous metal or polymer-based hollow fibers were used as both cathodes for hydrogen evolution reaction (HER) and membranes for filtration (microfiltration or ultrafiltration) of treated water in MEC (Sapireddy et al., 2019, Werner et al., 2016, Katuri et al., 2014). Using these dual-function hollow fiber cathodes, it was possible to simultaneously recover clean water and energy from domestic wastewater in a single unit. An important finding from these studies was that these dual-function cathodes have a self-cleaning property attributed to the *in-situ* H<sub>2</sub> bubble formation on the cathode surface and other factors associated with HER, which significantly delayed the onset of cathode biofouling. However, manufacturing these dual-function hollow fiber cathodes for large scale applications is not feasible at the moment using existing membrane synthesis techniques. Ding et al. 2016 used a two-chamber MEC with polymeric hollow fiber membrane (HFM) unit submerged in the cathode chamber. Scaling up this two-chamber system is expensive because of adding a middle membrane (additional capital cost) to separate the anode from cathode, and it increases internal resistance and hence more voltage is needed (operational cost) to drive the process. Alternatively, coupling a single chamber MEC with membrane filtration is more economical, and it should be studied with

an efficient fouling-control method as GAC fluidization, which has proven to control fouling in AnMBR with minimal energy requirements.

In this study, we developed and examined a novel AnEMBR configuration by coupling single-chamber MEC with Anaerobic Fluidized Membrane Bioreactors (AnFMBR). The new reactor configuration aimed at mitigating fouling by enclosing the HFM and GAC fluidization in an internal cylinder. The new AnFMBR-MEC system was tested to assess its kinetics and effectiveness in treating an acetate rich synthetic medium effective for EAB growth at room temperature (20-25°C). The performance of this reactor was quantified in terms of biogas production, substrate degradation and removal efficiency, membrane fouling, and microbial ecology compared with an AnFMBR under the same operating conditions.

## CHAPTER II

### MATERIALS AND METHODS

#### A. Reactor configuration

The Two tubular laboratory-scale bioreactors (AnFMBR and AnFMBR-MEC) were constructed from Plexiglas-material, with a 1.5 L total volume and an effective volume of 1.43 L (Figure 1). Each reactor has a height of 50 cm, a diameter of 6.4 cm and contained an inner tube of 3.5 cm diameter. The inner tube was perforated with 5 mm holes at the top to allow fluid flow between the inner and outer tube. A polyvinylidene difluoride (PVDF) hollow fiber membranes of 0.00575 m<sup>2</sup> total surface (50 cm height, 0.1 μm pore size, 0.8 mm inner diameter, and 2 mm outside diameter) (Kolon Inc., South Korea) was submerged in the inner tube with 55 g of GAC (Calgon Carbon, Catalog # 207C, USA), and connected to a peristaltic pump (model no. 7528-30, Masterflex, Vernon Hills, IL) providing a constant effluent of 1L/day. The GAC was used as a carrier for microbial colonization and to minimize fouling by fluidization with a 60-70% bed expansion achieved at a recirculation rate of 0.75 L/min. The AnFMBR-MEC electrodes (i.e., anode and cathode) were placed in the outer tube and were connected with titanium wires (200 μm diameter, goodfellow, UK) to an external power source (3645A, DC Power supply, Circuit Specialists.INC, USA). The carbon-cloth anode (CC4P, Fuel cell earth, USA) and nickel mesh cathode (Guangzhou Kavatar Trading Co. Ltd) had an area of 427.5 cm<sup>2</sup> and 344 cm<sup>2</sup>, respectively (Figure 2).

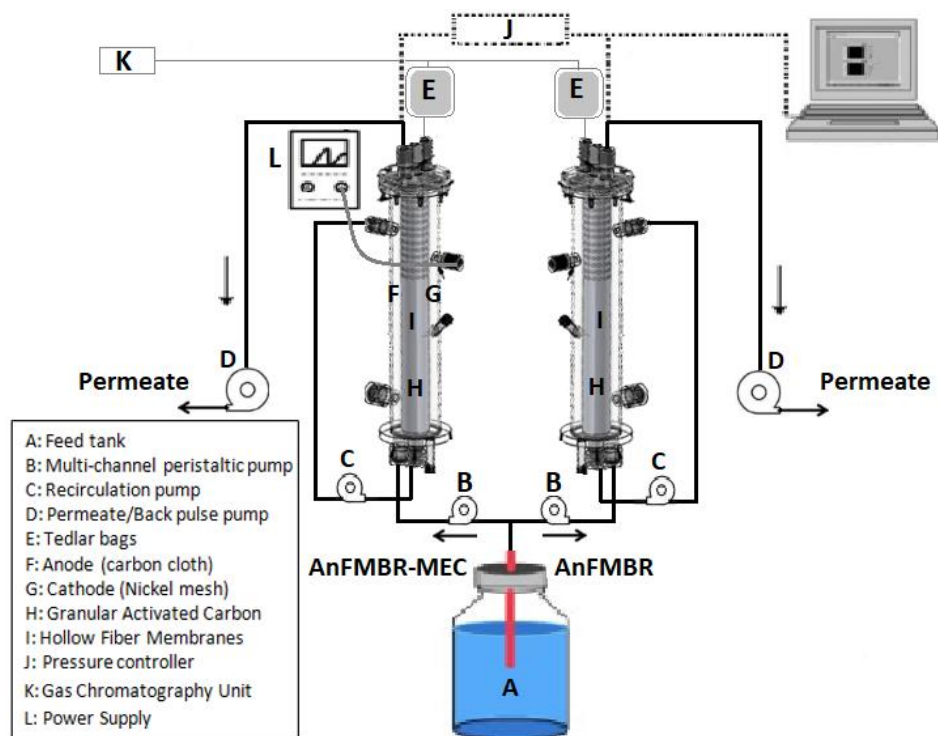


Figure 1: AnFMBR MEC and AnFMBR Setup

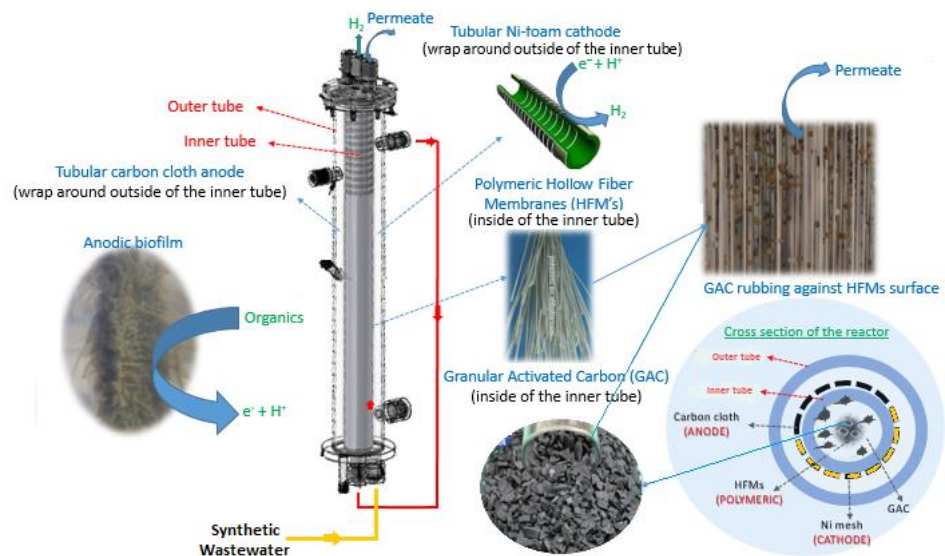


Figure 2: Detailed reactor configuration of AnFMBR-MEC

## **B. Reactor Start-up and Operation**

The two reactors were operated in parallel at room temperature (20-25°C). They were inoculated on day 1 with 1 L of cow manure solution (500 g fresh cow manure with 2 L of distilled water) and then later with a sludge collected from an existing AnMBR reactor. The AnFMBR was inoculated on day 2 and 17 with 70 and 50 mL of sludge, respectively. Whereas, the AnFMBR-MEC system was inoculated with a lower volume of sludge (10 mL) on day 7 because EAB adapt faster than methanogens (Katuri et al., 2014). The synthetic wastewater tank was purged with nitrogen gas of high purity (99.99%) for around 30 minutes to ensure an anaerobic atmosphere, and then stored at 4°C in the dark to avoid microbial growth. Following start-up period (87 days), sodium acetate concentration was lowered from 0.82 g/L (start-up phase) to 0.6 g/L (to mimic COD concentration close to low-organic strength wastewater, i.e., 0.4 g/L COD) for the remaining operation period. During the start-up and operation period, the reactors were continuously fed with a synthetic medium (Table 1) at a fixed hydraulic retention time (HRT) of 1.5 days.

## **C. Analysis**

### ***1. COD and biogas analysis***

Effluent samples were collected 2-3 times per week, filtered through 0.2 µm pore diameter syringe filters (polytetrafluoroethylene, PTFE, 13 mm size, Kinesis LTd) and stored at -20°C to be consequently analyzed for soluble COD using the Standard Method 5220 D (Hach company, Loveland, CO). Gas analysis was also conducted 2-3 times per week by collecting 200 µl sample volume from the reactor headspace and gas bags (Calibrated Instruments Inc.) and analyzing it using an SRI 310C Gas Chromatograph

(GC). The GC columns were a 6' Molecular Sieve, 3' Silica Gel, and a 3' HayesSep D with argon as carrier gas to detect hydrogen, nitrogen, methane and carbon dioxide volumes. Gas and COD readings were presented as average of weekly data.

Table 1: Synthetic wastewater composition (Wang et al., 2013, Katuri et al., 2010)

Composition	Concentration
Ammonium Chloride (NH <sub>4</sub> Cl)	1.5 g/L
Sodium Phosphate Dibasic (Na <sub>2</sub> HPO <sub>4</sub> )	0.6 g/L
Potassium Chloride (KCl)	0.1 g/L
Sodium Acetate (C <sub>2</sub> H <sub>3</sub> NaO <sub>2</sub> )	0.82 or 0.6 g/L
Sodium Bicarbonate (Na <sub>2</sub> HCO <sub>3</sub> )	2.5 g/L
Trace Elements <sup>a</sup>	10 ml/L
Vitamin Solution <sup>b</sup>	10 ml/L

<sup>a</sup> Composition of the Trace Elements solution (in g/L): Nitrilotriacetic acid:1.50, MgSO<sub>4</sub>·7H<sub>2</sub>O:3.00, MgSO<sub>4</sub>·H<sub>2</sub>O:0.50, NaCl:1.00, FeSO<sub>4</sub>·7H<sub>2</sub>O:0.10, CoSO<sub>4</sub>·7H<sub>2</sub>O:0.18, CaCl<sub>2</sub>·2H<sub>2</sub>O:0.10, ZnSO<sub>4</sub>·7H<sub>2</sub>O:0.18, CuSO<sub>4</sub>·5H<sub>2</sub>O:0.01, KAl(SO<sub>4</sub>)<sub>2</sub>·12H<sub>2</sub>O:0.02, H<sub>3</sub>BO<sub>3</sub>:0.01, Na<sub>2</sub>MoO<sub>4</sub>·2H<sub>2</sub>O:0.01, NiCl<sub>2</sub>·6H<sub>2</sub>O:0.03, Na<sub>2</sub>SeO<sub>3</sub>·5H<sub>2</sub>O:0.3mg, Distilled water:1000mL <sup>b</sup> Composition of the Vitamin solution (in mg/L): Biotin:2.00, Folic acid:2.00, Pyridoxine:10.00, Thiamine-HCl·2H<sub>2</sub>O:5.00, Riboflavin:5.00, Nicotinic acid:5.00, D-Ca-pantothenate:5.00, Vitamin B12:0.10, p-Aminobenzoic acid:5.00, Lipoic acid: 5.00, Distilled water: 1000mL

## 2. Scanning Electron Microscopy (SEM)

At the end of the experimental period, samples from the fouled and virgin HFM were taken and stored overnight in a glutaraldehyde fixative solution (2 % in 50 mM phosphate buffer, pH 7.0). After fixation, the samples were dehydrated using a series of graded alcohol solutions (10 to 100%; 10 min at each dilution). Then, an oven was used to dry the samples for 30 min at 30 °C. Dried samples were fixed on an aluminum stub with double-sided copper tape. Prior to SEM imaging (Quanta 600) in an argon atmosphere, the samples were sputter-coated with iridium layer (5 nm thick) for 40 s at 25 mA current (Quorum

Q150T ES). Finally, the samples were examined at an accelerating voltage of 5 KV at a spot size of 3 and beam current of 3  $\mu$ A.

### ***3. DNA extraction, Library preparation, sequence and analysis***

DNA Samples for microbial community analysis were collected from the suspension, GAC, HFM and electrodes, and then stored at - 20°C. DNA was extracted from the samples using a standard protocol for FastDNA Spin kit for Soil (MP Biomedicals, USA) with the subsequent modifications; 500 L of sample, 480 L Sodium Phosphate Buffer and 120 L MT Buffer were added to a Lysing Matrix E tube. Bead beating was performed at 6 m/s for 4 x at 40s each (Albertsen et al., 2015). Gel electrophoresis using TapeStation 2200 and Genomic DNA screentapes (Agilent, USA) was used to validate product size and purity of a subset of DNA extracts. DNA concentration was measured using Qubit dsDNA HS/BR Assay kit (Thermo Fisher Scientific, USA).

The bacterial and archaeal 16S rRNA gene region V4 sequencing libraries were prepared by a custom protocol based on an Illumina protocol and the purified sequencing libraries were paired-end sequenced (2x300 bp) on a MiSeq™ (Illumina, USA) using a MiSeq Reagent kit v3 (Illumina, USA) following the standard guidelines for preparing and loading samples on the MiSeq. Details of the sequencing library preparation are provided in the Appendix A.

Forward and reverse reads were trimmed for quality using Trimmomatic v. 0.32 (Bolger et al., 2014) with the settings SLIDINGWINDOW:5:3 and MINLEN: 225. The results were analyzed in R v. 3.5.1 (R Core Team, 2017) through the Rstudio IDE using the ampvis



package v.2.4.10 (Albertsen et al., 2015). The trimmed reads were dereplicated and formatted for use in the UPARSE workflow (Edgar, 2013). The dereplicated reads were clustered, using the usearch v. 7.0.1090 -cluster\_otus command with default settings. Operational taxonomic unit (OTU) abundances were estimated using the usearch v. 7.0.1090 -usearch\_global command with -id 0.97 -maxaccepts 0 -maxrejects 0. Taxonomy was assigned using the RDP classifier as implemented in the parallel\_assign\_taxonomy\_rdp.py script in QIIME (Caporaso et al., 2010), using -confidence 0.8 and the SILVA database, release 132 (Quast et al., 2012). The results were examined in R v. 3.6.0 (R Core Team, 2017) through the Rstudio IDE using the ampvis package v.2.4.10 (Albertsen et al., 2015).

#### ***4. Voltage and transmembrane pressure (TMP) measurements***

The TMP in both reactors was measured with a pressure transducer from Cole Parmer and recorded every 10 seconds using a data acquisition device (LabJack U6, LabJack Corporation, Lakewood, CO). An external power source (CSI3645A) was used to apply voltage to the circuit, and a high resolution PicoLog data logger was used to measure the voltage across the electrodes in the AFMBR-MEC every 30 minutes. Using ohm's law ( $I=V/R$ ), and at a constant resistance of  $10 \Omega$ , the current was calculated from the measured voltage and consequently Coulombic efficiency (CE) was calculated according to Katuri et al. (2014) to quantify the electrochemical performance of the system. At the end of the experiment, a reference electrode [Ag/AgCl (3M NaCl) Reference Electrode; BASi] was inserted in the AnFMBR-MEC from the closest port to the anode and cathode to measure their potentials.

### 5. Energy Requirements and Production

Assessment of the energy consumption, recovery and efficiency was conducted in accordance to a common approach reported for MEC applications (Katuri et al., 2014, Cusick et al., 2011). As such, the energy consumption ( $W_e$ ) from recirculation and filtration provided by the pumps (in both reactors) and due to power supply in the AnFMBR-MEC adjusted for losses across the resistor was calculated using Equation 1.

$$W_e(\text{Kwh}) = \left( \frac{Q_1 \delta E_1 + Q_2 \delta E_2}{\frac{1000}{Q_2}} \right) * V + \sum_1^n (I E_{ps} \Delta t - I^2 R_{ex} \Delta t) * 0.000278 \quad (1)$$

Where  $Q_1$  is the reactor recycle rate (m<sup>3</sup>/s),  $\delta$  is the unit weight of water which is 9800 N/m<sup>3</sup>,  $E_1$  is the measured hydraulic pressure head loss through the system (m),  $Q_2$  is the permeate flow rate (m<sup>3</sup>/s),  $E_2$  is the head loss due to TMP (m),  $V$  is the total volume pumped (m<sup>3</sup>),  $I$  is the current generated by the AnFMBR-MEC system (A),  $\Delta t$ (s) is the time increment for  $n$  data points measured during a cycle, and  $E_{ps}$  is the applied voltage from the power source (V),  $R_{ex}$  is the external resistor in the circuit ( $\Omega$ ), and 0.00278 is a conversion factor from kJ to kWh (1 kWh = 3600 kJ).

The energy produced ( $W_{gas}$ ) was determined from the methane yield in the AnFMBR and from both methane and hydrogen yields in the AnFMBR-MEC (Equation 2 and 3).

$$n = v/TR \quad (2)$$

$$W_{gas}(\text{kJ}) = nH_2\Delta H_2 + nCH_4\Delta H_4 \quad (3)$$

Where  $n$  is the number of moles produced ( $nH_2$  and  $nCH_4$ ),  $v$  is the volume of gas (L),  $T$  is the temperature (K),  $R$  is the gas constant (0.08206 L.atm/K.mol), and  $\Delta$  is the energy

content based on the heat of combustion ( $\Delta H_2$ : 285.83 kJ/mol and  $\Delta H_4$ : 891 kJ/mol).

$W_{Gas}$  was converted to kWh using a conversion factor of 0.000278.

The overall energy efficiency was calculated for both reactors using Equations 4.

$$\eta_e = W_{gas} / W_e \quad (4)$$

Where  $\eta_e$  is the energy efficiency relative to the electrical input. The cathodic recovery, which is the number of moles of methane and hydrogen actually produced relative to those that could be recovered from the measured current, was also calculated for AnFMBR-MEC system using Equations 5a and 5b.

$$\eta_{ce}(H_2) = \int_{t=0}^t \frac{I dt}{2 F} \quad \& \quad \eta_{ce}(CH_4) = \int_{t=0}^t \frac{I dt}{8 F} \quad (5a)$$

$$\eta_{cat}(H_2) = n_{H_2} / \eta_{ce}(H_2) \quad \& \quad \eta_{cat}(CH_4) = n_{CH_4} / \eta_{ce}(CH_4) \quad (5b)$$

Where  $\eta_{ce}(H_2)$  or  $\eta_{ce}(CH_4)$  is the number of moles that could be recovered from the measured current,  $F$  is Faraday's constant (96.485 C/mol),  $I$  is the current (A),  $dt$  is the time interval over which data were collected (s), 2 is the number of electrons per mole of hydrogen, 8 is the number of electrons per mole of methane,  $\eta_{cat}$  is the cathodic recovery, and  $n_{H_2}$  or  $n_{CH_4}$  is the number of moles hydrogen or methane that is actually recovered.

## CHAPTER III

### RESULTS AND DISCUSSION

#### A. Start-up phase

The two reactors inoculated with cow manure and sludge started operating simultaneously at an OLR of 0.43 Kg of substrate/m<sup>3</sup>.day. At first, since gas generation was relatively low, biogas samples were taken from the headspace until the volume and mass percentage of methane stabilized. Subsequently gas bags were analyzed to ensure that the system has reached stable performance in terms of methane production before starting with the comparative operation phase. The AnFMBR-MEC voltage attained a value of 50 mV on day 10, and then ranged between 50 and 80 mV from day 10 till 20. Subsequently, the voltage increased until day 40 when it stabilized at a value of  $\sim 307 \pm 83$  mV. Methane generation increased as well during this period and reached stability on day 40 with methane generation rate of  $0.2 \pm 0.004$  m<sup>3</sup>/m<sup>3</sup>/d ( $76.16 \pm 5.17\%$  by biogas volume), while hydrogen generation gradually decreased. The AnFMBR-MEC reactor reached stable performance (methane generation and voltage) after 40 days, while the AnFMBR reactors took 65 days to stabilize (methane generation). The difference in the stabilization of the system performance between the two reactors probably depended on the variance in the establishment of the microbial community. During the start-up stage (OLR: 0.43kg of substrate/m<sup>3</sup>.day), the AnFMBR's biogas yield was 0.277 L/g.COD removed while COD removal was 95%. As for AnFMBR-MEC, biogas yield was 0.203 L/g.COD removed and COD removal was 99%.

## **B. COD, biogas and electrochemical performance during operation phase**

Membrane The performance of the AnFMBR-MEC system was compared with the AnFMBR in terms of COD removal (Figure 3) and biogas generation (Figure 4). The OLR was lowered from 0.43 kg of substrate/m<sup>3</sup>.day (start-up phase) to 0.31 kg of substrate/m<sup>3</sup>.day (operation phase) by lowering the acetate concentration from 0.82 g/L to 0.6 g/L and keeping the HRT fixed at 1.5 days. During the operation phase, the AnFMBR COD removal was not affected for the first few days but after one week and for a period of 6 weeks, COD removal dropped and was varying between 9-74% (Figure 3). This drop in performance can be attributed to the time needed for the microbial community to adapt to the new OLR. The AnFMBR fully recovered after 6 weeks and the COD removal was in the range of 80-98% with an average of 90% (Figure 3). After the long time needed for the microbial community to adapt to the new OLR and the further decrease in performance that happened due to a fluidization problem on week 16 (decrease in water level, forcing GAC particles to flow from inner tube to outer tube and blocking pumps tubing; resolving this problem caused loss of some fluid, GAC and therefore, loss of microbial communities), a relatively stable methane yield was observed at an average of 0.128 L/g. COD removed from week 21 onward (Figure 4). As for the AnFMBR-MEC, a fluidization problem occurred immediately on the first few days of operation and affected the performance of the reactor, causing a significant drop in COD removal (Figure 3). The COD removal started to increase reaching 32% after one week and a high treatment efficiency was attained after 8 weeks with COD removal values between 49 and 76%. From week 12 of operation until the end of the experiment (week 27) the removal remained between 84-95% (Figure 3). In

terms of biogas production, the AnFMBR-MEC reactor recovered completely after 6 weeks yielding 0.31 L/g.COD removed (Figure 4).

While traces of H<sub>2</sub> were observed in the AnFMBR-MEC at early stages of operation, methane was the dominant biogas. During the operation period prior to GAC removal (OLR: 0.31 kg of substrate/m<sup>3</sup>.day), CE values were in the range of 40.92±10.23%, with an average volumetric current density of 22.19±5.48 A/m<sup>3</sup> (0.97±0.24 A/m<sup>2</sup>) and cathodic recovery of 36.52±21.42% (Figure 5, Table2). However, during the last 16 days of this period (days 59-74), CE values dropped to an average of 24.43%, and similarly the current density (13.18 A/m<sup>3</sup> or 0.57 A/m<sup>2</sup>). A recent study investigating the effect of configuration and applied voltage on performance showed that the tubular reactor configuration has lower CE values (<60%) than the rectangular configuration (>83%) at 0.7V, and that the CE decreased with time of operation with an acetate-based medium, with higher fraction of electrons lost to other processes at 0.7V than at 0.9V (Werner et al., 2016). The low value of CE attained in AnFMBR-MEC after 59 days of operation indicated that only around quarter of the electrons from the acetate oxidization were transferred to the anode. The other fraction of electrons were involved in alternative metabolisms as methanogenesis, fermentation and biological direct interspecies electron transfer (DIET) (Feng et al., 2018, Tian et al., 2015). The high electrical conductivity of GAC particles is hypothesized to have stimulated DIET between *Geobacter* and methanogens and thus favored methane production (Aslam et al., 2018, Liu et al., 2012), and this was manifested in the microbial community analysis below which showed high relative abundances of *Geobacter* and *Methanosarcina* on GAC. Due to this drop in CE, the GAC was removed on day 74 of

operation to study its effect on the AnFMBR-MEC performance, and therefore the system was operated as AnMBR-MEC (i.e., no GAC and fluidization) with a new feed (fluid was completely replaced) for the remainder of the experiment. Upon GAC removal, biogas yield dropped instantly but then increased after one week thereafter supporting the resilience of the AnFMBR-MEC system. For the next three months following GAC removal, methane yield had an average of  $0.2 \pm 0.047$  and a maximum of  $0.25$  L/g.COD removed (Figure 4), and methane generation rate was  $0.031 \pm 0.014$  m<sup>3</sup>/m<sup>3</sup>/d (Table 2). The AnMBR-MEC recovered higher electrical current than before ( $r_{\text{cat}}$ :  $57.58 \pm 27.96\%$ ), however, the CE ( $25.26 \pm 6.72$ ) and volumetric current density ( $13.60 \pm 3.64$  A/m<sup>3</sup>) values were not affected by GAC removal and maintained the same ranges as the last 16 days of first period (i.e., prior to GAC removal) of operation.

During the first period of operation (i.e., prior to GAC removal) of AnFMBR-MEC, we observed breakage of GAC due to fluidization producing fine particles (black color observed in the reactor) that have attached to the membrane, reactor surface and electrodes. These fine particles were able to flow to the outer tube and might have disrupted the anodic microbial community. The higher methane rate ( $0.031 \pm 0.014$  m<sup>3</sup>/m<sup>3</sup>/d) observed during the second period of operation (i.e., after removal of GAC) was mainly attributed to the indirect contribution of these fine GAC particles to methane generation as similar abundances of *Geobacter* and *Methanosarcina* were observed between samples of GAC (before removal from reactor) and the HFM collected at the end of the experiment (GAC was not present at this time). At the end of operation, the measured anode and cathode potentials were  $-0.3$  and  $-1.0$  V vs. Ag/AgCl, respectively.

In general, both reactors had a good treatment performance with high COD removal around 90% during stable operation. However, the methane yield of AnFMBR-MEC was 56% higher than that of the AnFMBR during the last 7 weeks of stable operation. Table 3 further highlights the AnFMBR-MEC system advantages by comparing its results during stable operation to those of the AnFMBR.

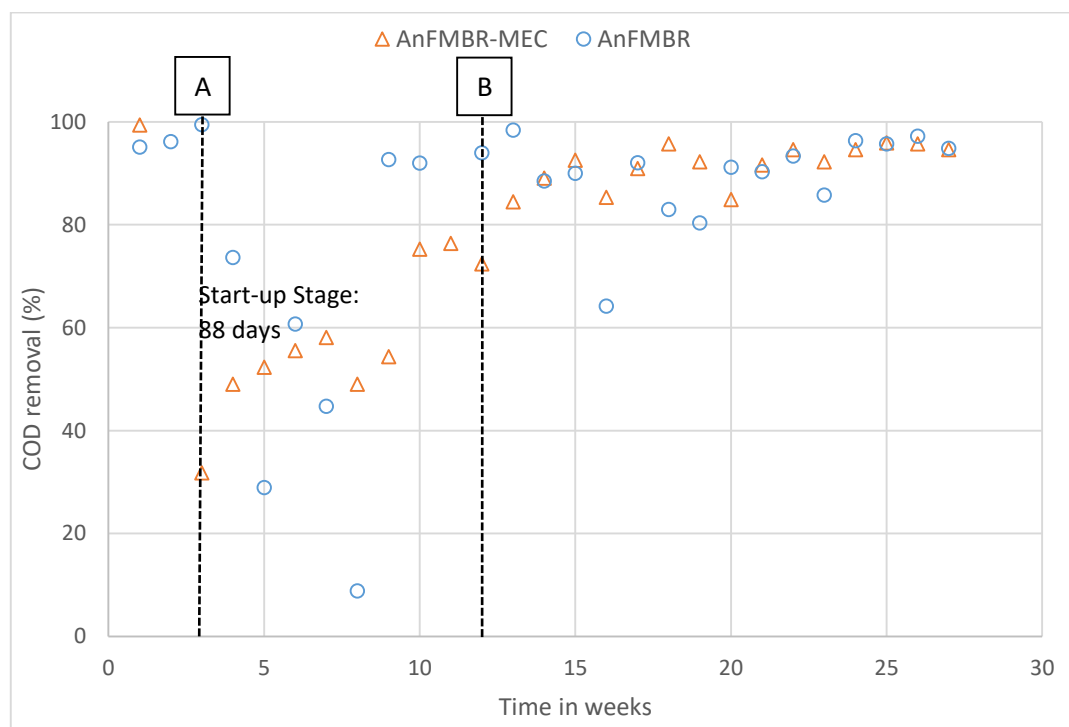


Figure 3: COD removal (weekly average) in both reactors during operation phase. (A: OLR change in both reactors, and fluidization problem occurrence in the AnFMBR-MEC- the fluidization problem refers to a decrease in water level, forcing GAC particles to flow from inner tube to outer tube and blocking pumps tubing; resolving this problem caused loss of some fluid, GAC and therefore, loss of microbial communities- B: GAC removal in the AnFMBR-MEC after CE drop)



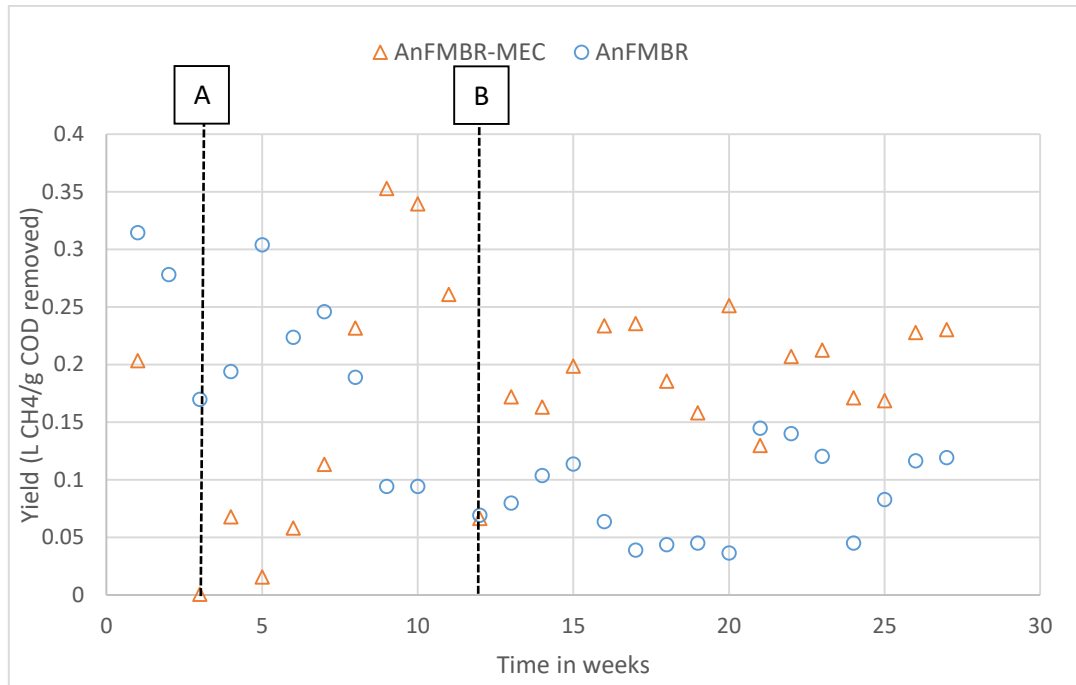


Figure 4: Methane yields (average weekly) for both reactors during operation phase. (A: OLR change in both reactors, and fluidization problem occurrence in the AnFMBR-MEC- the fluidization problem refers to a decrease in water level, forcing GAC particles to flow from inner tube to outer tube and blocking pumps tubing; resolving this problem caused loss of some fluid, GAC and therefore, loss of microbial communities- B: GAC removal in the AnFMBR-MEC after CE drop)

Table 2: Performance of the AnFMBR-MEC

Voltage	OLR (kg /m <sup>3</sup> .day )	CH <sub>4</sub> rate (m <sup>3</sup> /m <sup>3</sup> /day)	CE (%)	r <sub>cat</sub> (%)	Current density (A/m <sup>3</sup> )	Current density (A/m <sup>2</sup> )
0.7 <sup>a</sup>	0.43	0.050	37.24	76.53	22.41±2.73	0.98±0.12
0.7 <sup>b</sup>	0.31	0.024±0.017	40.92±10.23	36.52±21.42	22.19±5.48	0.97±0.24
0.7 <sup>c</sup>	0.31	0.031±0.014	25.26±6.72	57.58±27.96	13.60±3.64	0.59±0.16

<sup>a</sup> Average values of first three days of operation with GAC fluidization immediately after startup at an OLR of 0.43 kg of substrate/m<sup>3</sup>.day.

<sup>b</sup> Average values of first operation period with GAC fluidization at an OLR of 0.31 kg of substrate/m<sup>3</sup>.day.

<sup>c</sup> Average values of second operation period after GAC removal at an OLR of 0.31 kg of substrate/m<sup>3</sup>.day

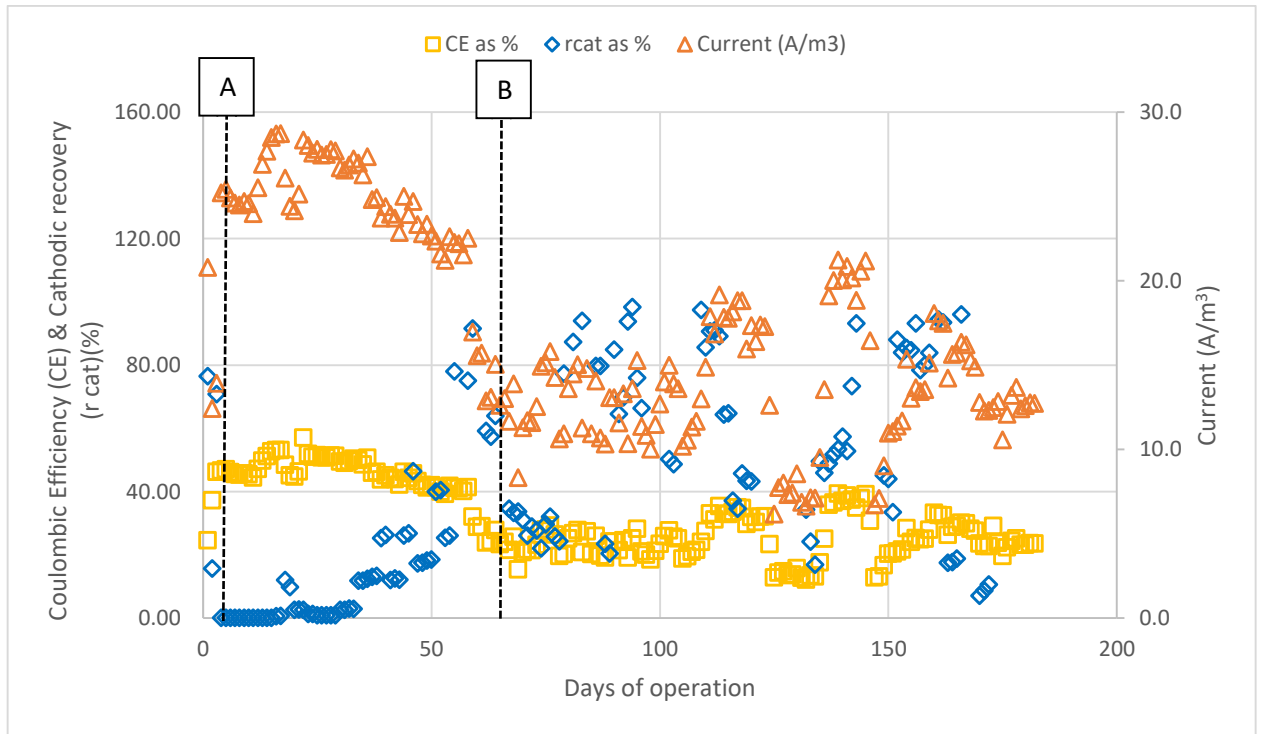


Figure 5: Electrochemical performance of the AnFMBR-MEC during operation phase. (A: OLR change in both reactors, and fluidization problem occurrence in the AnFMBR-MEC- the fluidization problem refers to a decrease in water level, forcing GAC particles to flow from inner tube to outer tube and blocking pumps tubing; resolving this problem caused loss of some fluid, GAC and therefore, loss of microbial communities- B: GAC removal in the AnFMBR-MEC after CE drop)

### C. Fouling during operation phase

Since fouling is one of the major limitations in anaerobic membrane processes, the TMP of both reactors was continuously monitored (Figure 6). After the start-up period, the TMP for the AnFMBR-MEC was around 4-5 KPa, and it remained stable until day 74 of operation phase. After the GAC removal on day 74, the TMP gradually increased by 2-3 folds, remaining in the range of 8-12 KPa. Alternatively, the AnFMBR reactor fouled faster than that of AnFMBR-MEC system. The TMP of the AnFMBR reactor was around 5 KPa after the start-up period and increased slightly to reach 10 KPa at day 47 of operation phase. It remained stable till day 94, then started to increase to reach 78 KPa at the end of

the experiment (day 182). It can be concluded that the AnFMBR-MEC offered an advantage over the AnFMBR since both reactors had the same membrane flux of 6.5 LMH, and same configuration and operating conditions.

Table 3: Comparison between AnFMBR and AnFMBR-MEC during stable performance

	AnFMBR-MEC	AnFMBR
Resistor ( $\Omega$ )	10	10
Applied Voltage (V)	0.7	0.7
Temperature ( $^{\circ}\text{C}$ )	20-30	20-30
Substrate	Synthetic	Synthetic
Working volume (L)	1.43	1.43
COD feed (mg/L)	463	463
COD removal (%)	85-96	80-97
CH <sub>4</sub> volume percentage in biogas (%)	80	63
CH <sub>4</sub> average yield (L/g.COD removed)	0.2	0.128
pH (Feed)	~7	~7
Organic Loading Rate (OLR)	0.43	0.43
Permeate Flux LMH (L/m <sup>2</sup> /h)	6.5	6.5
Average volumetric current density (A/m <sup>3</sup> )	13.8	-
CE (%)	25.26	-
$r_{\text{cat}} \text{CH}_4$ (%)	57.58	-
CH <sub>4</sub> rate (m <sup>3</sup> /m <sup>3</sup> /d)	0.031	0.01585
Fouling (KPa)	8-12	65.7-76.7
Energy required (KWh/m <sup>3</sup> )	0.131	0.069

Membrane fouling mitigation by electrical fields have proven to be effective due to the electric repulsive forces driving foulants away from the membrane and retarding their attachment (Tian et al., 2015, Akamatsu et al., 2010). Additionally, a simple speculation on the fouling behavior in this study is based on the electron balance. In the AnFMBR-MEC we have many separated parts for biomass formation, and the electrons in acetate have possibly resulted in biomass synthesis for anode biofilm, cathode biofilm, and biofilm on

reactor walls, hence lowering the suspended solids in suspension, and alleviating membrane fouling (Gkotsis and Zouboulis, 2019). However, further studies are needed to expound fouling in this AnFMBR-MEC configuration and to study the relationship between GAC fluidization and fouling propensity, especially when removing GAC from mid-operation, since no previous work has tested it before.

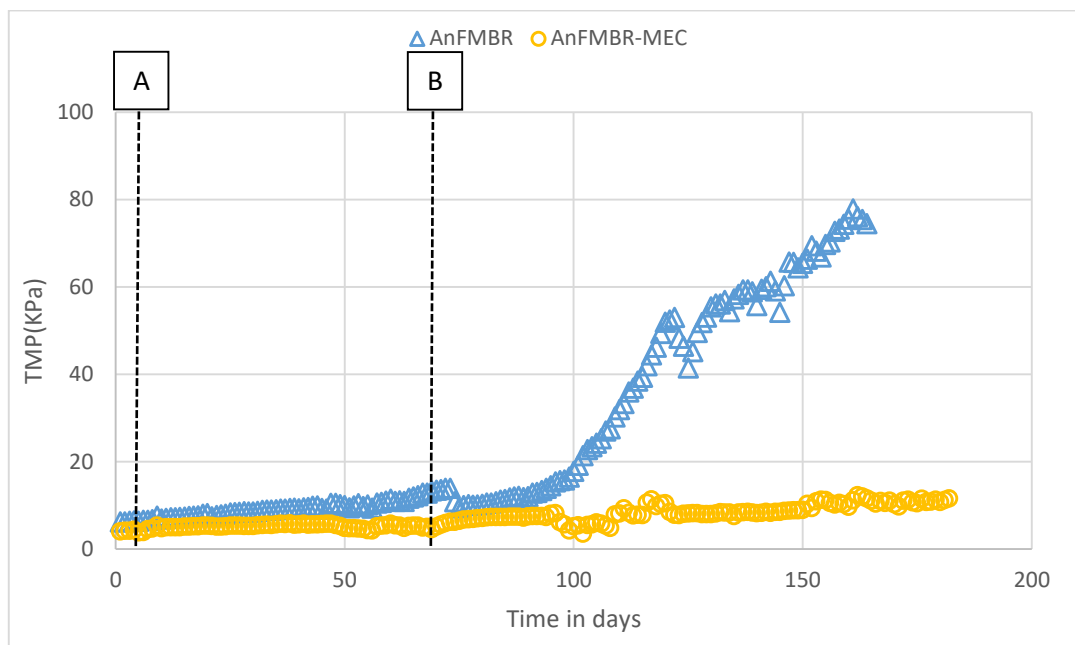


Figure 6: Transmembrane pressure (TMP) values during operation phase. (A: OLR change in both reactors, and fluidization problem occurrence in the AnFMBR-MEC- the fluidization problem refers to a decrease in water level, forcing GAC particles to flow from inner tube to outer tube and blocking pumps tubing; resolving this problem caused loss of some fluid, GAC and therefore, loss of microbial communities- B: GAC removal in the AnFMBR-MEC after CE drop)

#### **D. Energy balance.**

While the energy demand for the AnFMBR is due to the operation of pumps for recirculation and filtration, the largest fraction of energy consumption for the AnMBR-MEC system was attributed to the power supplied to drive electrochemical reactions. The total energy demand was on average 0.3 and 0.22 kWh/m<sup>3</sup> for the AnFMBR-MEC before and after GAC removal respectively (including energy for power source and pumps), and 0.12 kWh/m<sup>3</sup> for AnFMBR. Using the number of moles of CH<sub>4</sub> produced per day and the higher heating values for methane ( 890 kJ/mol), the energy recovered from methane was estimated at 0.25 kWh/m<sup>3</sup> (before GAC removal) and 0.32 kWh/m<sup>3</sup> (after GAC removal) for the AnFMBR-MEC and 0.18 kWh/m<sup>3</sup> for AnFMBR. Since the efficiency of methane recovery to electricity is 33% (Katuri et al, 2014; Kim et al, 2011), the maximum electricity that could be generated was 0.08 kWh/m<sup>3</sup> (before GAC removal) and 0.1 kWh/m<sup>3</sup> (after GAC removal) for AnFMBR-MEC, and 0.06 kWh/m<sup>3</sup> for the AnFMBR. Based on the total energy demand and the energy recovered from methane, the net energy needed to operate the reactors was estimated at 0.22 kWh/m<sup>3</sup> (before GAC removal) and 0.12 kWh/m<sup>3</sup> (after GAC removal) for the AnFMBR-MEC and 0.06 kWh/m<sup>3</sup> for the AnFMBR, less than reported values for anaerobic processes (0.25-1.00 kWh/m<sup>3</sup>) (Liao et al., 2006, Kim et al., 2011). Although the energy required for the AnFMBR was less than that of the AnFMBR-MEC, the latter recovered greater methane with less fouling potential which is the main disadvantage of the AnMBR system as it requires much energy for cleaning through backwashing or costs associated with chemical cleaning or membrane replacement. Furthermore, the low applied voltage of 0.7 V can be supplemented with a renewable energy such as solar energy (Katuri et al., 2019).

## E. Microbial Community.

The Biomass samples from suspension, GAC, HFM, and electrodes were collected from both reactors for microbial community characterization at different time intervals. The inoculum (i.e., cow manure and sludge) used to start the reactors was rich with *Firmicutes* (24.4%), *Actinobacteria* (12.3%) and the genus *Methanobacterium* (5.2%), a hydrogenotrophic methanogen (Figure 7). To examine the enrichment of process-critical microbes from the inoculum, the first sampling occurred on day 5 of operation, and it revealed the presence of *Desulfuromonas* and *Geobacter* (a known genus with members capable of electricigenesis) on the AnFMBR GAC (3.1% and 24.3%, respectively). *Methanosarcina* was also detected to be dominant on AnFMBR GAC (10.7%) and in suspension (23.4%). For the AnFMBR-MEC, *Desulfuromonadales* (20.9%), *Geobacter* (9.4%), and *Desulfovibrio* (3.7%) had high relative abundances on the GAC with *Methanosarcina* being also most abundant in suspension (39.6%). Some members of the genus *Geobacter* are known for their ability to directly transfer electrons, through DIET, to methanogens on GAC and therefore reducing CO<sub>2</sub> to CH<sub>4</sub> (Zhao et al., 2015, Reguera et al., 2005). EAB belonging to *Desulfuromonas* and *Pseudomonas*, can also enable DIET with methanogens (Barua et al., 2019, Lin et al., 2017), and *Desulfuromonas* in particular can assist the transfer of electrons by producing conductive nanowires (Reimers et al., 2017). The co-existence of *Methanosarcina* with EAB on GAC suggests the possibility of DIET occurring between EAB and acetoclastic methanogens which are capable of direct uptake of electrons (Park et al., 2018a, Park et al., 2018b, R. Lovley, 2017, Cheng and Call, 2016, Rotaru et al., 2014a, Rotaru et al., 2014b). Among the genera of methanogens, *Methanosaeta* and *Methanosarcina* are the only methanogens with membrane-bound cytochromes (Thauer et al., 2008), capable of playing a role in extracellular electron exchange (Rotaru et al., 2014c). In this

process, the electrically conductive pili and outer surface cytochromes appear to be very important for DIET, specifically for *Geobacter* species (Lovley, 2012, Lovley et al., 2011).

	AnFMBR						AnFMBR-MEC								
Euryarchaeota; Methanosarcina	1.6	25.4	0.9	5.5	10.7	8.1	10	38.6	12.8	26.1	1	1.4	8.8	7.2	4.9
Deltaproteobacteria; Geobacter	0	3.3	11.1	0.2	24.3	6.5	0.2	1.6	4.7	2.2	5.5	9.4	2.2	1.1	10.2
Bacteroidetes; f_WCHB1-69_OTU_2	0	5.9	4.9	2.4	8	6.2	4.6	4.3	8.8	7.3	6.5	3.5	4.5	2	5.4
Bacteroidetes; vadinBC27 wastewater-sludge group	0	4.6	4.7	8.4	5.6	3.2	2.4	1.6	3.8	1.2	4.9	1.6	1.2	2	6.5
Betaproteobacteria; f_Rhodocyclaceae_OTU_5	0	3.4	2.6	1.2	3.6	1.6	0.7	7.7	3.1	2.2	2.2	12.5	1.3	1.2	3.5
Synergistetes; f_Synergistaceae_OTU_11	0.9	2.5	4.8	1.5	5.2	4.7	3.9	2.9	2.2	4.2	3.8	2.7	0.9	0.7	5.2
Euryarchaeota; Methanoseta	0.9	0.9	1.3	4	0	0.4	14.1	0	0.8	2.1	1.7	0	0.9	10.4	1.4
Deltaproteobacteria; Desulfovibrio	0	2	0.2	0.2	3.9	1.9	0.4	2.3	1.1	1.3	0.3	3.7	9.5	3.2	2.1
Firmicutes; f_Family XI_OTU_7	0	3.3	1.6	0.6	4.8	3.6	0.2	0.1	3.9	2.6	3.3	0	1.3	4.5	2.1
Euryarchaeota; Methanobacterium	5.2	0.2	0.2	0.9	0.2	0.1	1.9	1.3	1.4	1.6	10.3	1.7	0.9	0.8	5.1
Deltaproteobacteria; o_Desulfuromonadales_OTU_18	0	0.1	0.1	0	0	3.9	0	1.5	1	0.6	0.4	20.9	0.6	0.3	0.1
Synergistetes; f_Synergistaceae_OTU_9	2.8	1.5	0.7	0.8	0.7	0.4	0.5	1.1	3.8	1.3	4.9	1.2	0.9	0.4	7.1
Deltaproteobacteria; Desulfuromonas	0	0	1.3	0	3.1	18.5	0.1	0.1	0	0.1	1.3	1	0	0.2	0.1
Spirochaetae; f_Spirochaetaeae_OTU_13	0	1.8	1.4	0.1	3.7	0.9	0.1	2.2	3	1.5	0.5	1.6	3	1.1	5.2
Actinobacteria; Corynebacterium 1	0.4	1.9	1.9	3.2	0.1	0.4	0.3	7	3.3	2.4	1.8	1	0.6	1	0.1
Betaproteobacteria; Advenella	0	5.7	0.1	0	0.2	0	0.5	0.2	6.3	2.4	0.6	0	2.7	2.6	1.2
Firmicutes; Turicibacter	3.9	0	0.1	0.2	0.1	0.1	0.6	0.2	0.2	0.6	0.3	0.1	6.3	10.7	0.1
Gammaproteobacteria; Acinetobacter	0.6	1.1	1.6	14.2	0.3	0.4	0.1	0.4	1.1	0.4	0.2	0.1	0.4	0.8	0
Firmicutes; f_Peptostreptococaceae_OTU_14	4.6	0	0.2	0.2	0.2	0.5	0.5	0.1	0.3	0.5	0.2	0.4	5.1	7.3	0.1
Gammaproteobacteria; f_Pseudomonadaceae_OTU_29	0	0.2	0.6	0.1	0.1	0.7	0	4.4	2.3	0.6	0.1	9.3	0.3	0.1	0.1
Actinobacteria; Actinotalea	0	0.5	1.6	0.9	1.6	2.3	0.7	0.6	0.9	0.8	2.9	5.3	0.2	0.2	0.4
Bacteroidetes; f_WCHB1-69_OTU_291	0	0.2	0	0.1	0.1	0.1	0.1	1.6	3.4	3.1	4.3	1.2	1.2	1.5	1.8
Actinobacteria; f_Propionibacteriaceae_OTU_15	0	0.2	12.7	1.1	0.1	0.7	0.1	0.1	0.2	0.1	1.1	0.2	0	0	0.3
Gammaproteobacteria; Pseudomonas	0	0.8	1.2	0.4	0.4	0.7	0.5	2	3.2	0.7	0.7	1.4	0.8	0.7	1.8
Synergistetes; Aminivibrio	0.1	0.9	2.4	1.5	0.5	1.2	3.9	0.4	0.3	0.8	1	0.3	0.2	0.1	0.8
Firmicutes; Christensenellaceae R-7 group	1.8	0.9	0.6	0.3	0.6	0.3	0.6	0.4	0.9	0.9	4.1	0.6	0.9	0.7	0.7
Bacteroidetes; Bivli28 wastewater-sludge group	0	0.7	0.2	0.2	0.3	0.9	0.9	0.5	1.1	2.7	0.1	0.1	5	0.4	1.2
Bacteroidetes; Petrimonas	0.2	0.3	1.7	2.2	0	0.3	4.7	0	0.2	0.5	1.8	0	0.2	0.3	0.7
Actinobacteria; Bifidobacterium	11.9	0	0	0	0	0	0	0.1	0	0	0	0	0.3	0.4	0
Firmicutes; Clostridium sensu stricto 1	3.5	0	0.2	0.2	0.1	0.1	0.5	0.2	0.3	0.6	0.3	0.3	2	3	0.1
Synergistetes; f_Synergistaceae_OTU_20	0	0.1	1.8	1.6	0	0.4	6.5	0	0	0	0.4	0	0	0	0.1
Spirochaetae; Treponema 2	1.2	0.3	0	0.4	0.1	0.1	1	0.4	0.2	0.7	0.2	0.1	4.9	1	0.2
Betaproteobacteria; f_Comamonadaceae_OTU_17	0.1	0.7	1.1	4.5	0.1	0.3	0.3	0.6	0.3	0.5	0.5	0.3	0.4	0.4	0.4
Chloroflexi; T78	1.4	0.5	0.3	0.1	1	0.6	1	0.1	0.4	0.8	1.4	0	0.3	0.6	0.4
Synergistetes; f_Synergistaceae_OTU_89	0	0	1	3.7	0	0.2	2.2	0	0.2	0.1	0.3	0	0.1	0.1	0.9
Firmicutes; Dethiosulfatibacter	0	0.6	0.7	0.1	0.1	0.9	0.8	0	1.3	1.2	1.1	0	0.4	0.7	0.7
Firmicutes; Peptoclostridium	2.8	0	0	0	0.2	0.1	0.2	0.1	0.1	0.2	0.1	0.4	1.9	2	0
Bacteroidetes; Proteiniphilum	0.5	0.5	1.7	0.7	0	0.4	1.4	0	0.3	0.1	0.8	0	0.3	0.2	0.9
Firmicutes; Family XIII UCG-002	0	0.4	0.2	0.3	0.5	0.9	0.3	0.8	1.1	0.5	0.4	0.3	0.3	0.4	1.4
Firmicutes; Ruminococcus 2	7.8	0	0	0	0	0	0	0	0	0	0	0	0	0	0
Inoculum															
Suspension_5 d															
Suspension_123 d															
Suspension_182 d															
GAC_5 d															
GAC_123 d															
HFM_182 d															
Suspension_5 d															
Suspension_74 d															
Suspension_123 d															
Suspension_182 d															
GAC_5 d															
Anode_182 d															
Cathode_182 d															
HFM_182 d															

Figure 7: The 40 most abundant genera (or lowest taxonomic classification level possible with f representing family level and o representing order level) in the AnFMBR and AnFMBR-MEC during the operation phase.

*Desulfovibrio* is a Sulfate-Reducing Bacteria (SRB) that facilitates direct electron transfer to the electrode (Kumar et al., 2017). Likewise, *Geobacter* plays an important role in transferring electrons directly from biodegradable organics to the anode (Yin et al., 2016). However, the relative abundance of *Geobacter* on the anode (2.2%) of AnFMBR-MEC was lower than GAC (9.4%) and HFM (10.2%). The low abundance of *Geobacter* in the anodic biofilm resulted in low CE of 31.7% and this suggests that electricigenesis might not be so effective in the presence of GAC in this AnFMBR-MEC configuration. GAC was reported to be a highly conductive

material that mimics the role of the conductive pili connecting EAB with the electrotrophic methanogenic archaea, *Methanosaeta* and *Methanosarcina* (Aslam et al., 2018, Feng et al., 2018, Liu et al., 2012). Since the relative abundance of *Geobacter* on GAC was accompanied with high relative abundance of *Methanosarcina*, this supports that DIET mechanism was possibly a dominant route for acetate consumption with methane generation. Generally, methane production in single-chamber MEC happens mostly due to hydrogenotrophic methanogens (*Methanobacterium*) on the cathode. However, *Methanosaeta* and *Methanosarcina* were more predominant than *Methanobacterium* on the cathode of AnFMBR-MEC. Two pathways of methane generation (direct or indirect through H<sub>2</sub>) could be mediated at the biocathode, one involving H<sub>2</sub> interspecies transfer (HIT), in which hydrogen generated from HER is oxidized into methane by carbon dioxide reduction by members of *Methanosarcina* (Lohner et al., 2014, Sieber et al., 2012) and the other one encompassing direct electron transfer from the cathode to methanogenic archaea (*Methanosaeta*) to reduce carbon dioxide into methane (Yee and Rotaru, 2020). Competition for hydrogen seemed to exist between Sulfate Reducing Bacteria (SRB) (*Desulfuivibrio*) and hydrogenotrophic methanogens on the cathode, further reducing their abundance. The SRB have high affinity for hydrogen, and their presence in anaerobic environments has been long proven to significantly reduce the abundance of hydrogenotrophic methanogens (Conrad, 1999).

In both reactors, *Bacteroidetes* and *Synergistetes* had high relative abundances in suspension and on HFMs which suggest that these fermenters may have contributed to HFM biofouling in both reactors due to the accumulation of dead-cell organics on the membrane surface during the filtration process (Ma et al., 2013). Methanogenic communities were abundant on the HFM with *Methanosaeta* (14.1%) and *Methanosarcina* (10.1%) dominant on the



AnFMBR HFM, and *Methanobacterium* (5.1%) and *Methanosarcina* (4.9%) on the AnFMBR-MEC HFM. In the AnFMBR, the acetoclastic methanogens (*Methanosaeta* and *Methanosarcina*) were highly abundant on HFM occupying around 24% of total microbial community deposited on the membrane. SEM was conducted at the end of operation for biofouled HFMs and for electrodes to characterize their surface structure after biofilm formation (Error! Reference source not found.). Cells with long filaments chains were observed in SEM images. *Methanosaeta sp.* were observed to form long filaments chains (Enzmann et al., 2018). The high TMP values (78 kPa) in the AnFMBR could be therefore attributed to the high relative abundance of *Methanosaeta sp.* on the HFM.

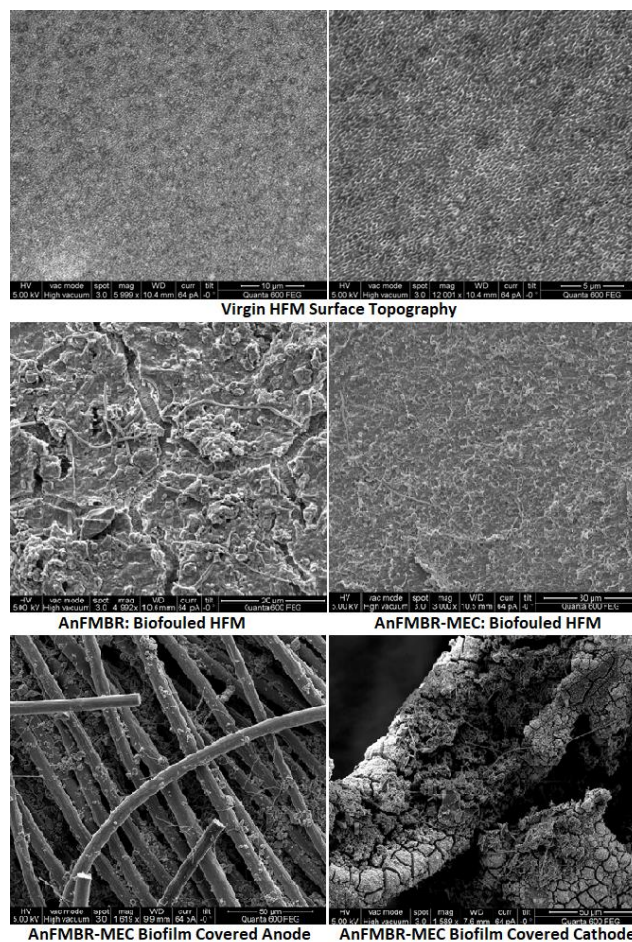


Figure 8: Virgin vs. biofouled HFM surface and biofilm covered anode and cathode.

## CHAPTER IV

### CONCLUSION

The performance of a new AnFMBR-MEC system was evaluated in a laboratory scale, at room temperature, with a continuous mode operation, and using a synthetic wastewater feed with a COD value of 470 mg/L. The novel system offered several advantages over the AnFMBR including a shorter start-up time (40 vs. 65 days), improved gas yield (0.2 vs 0.15 L/g.COD removed), and a more effective fouling mitigation (TMP of 12 vs. 78 Kpa after 264 days of operation) while achieving similar COD removal (~90%). Microbial community analysis suggests the occurrence of DIET between the EAB (mainly *Geobacter*) and *Methanosarcina* in both reactors. *Geobacter* species were mainly localized on the GAC and relatively less abundant on the anode demonstrating that electricigenesis might not be effective in this new configuration. Although, the AnFMBR-MEC (0.131 Kwh/m<sup>3</sup>) required higher energy than the AnFMBR (0.069 Kwh/m<sup>3</sup>), the energy needed for power supply is small and can be provided by a renewable energy source such as solar. Based on all these findings, it could be concluded that this system, coupling a single chamber MEC with membrane filtration and GAC fluidization, is economical and promising for the treatment of low strength wastewater. However, further studies are needed to examine the relationship between GAC fluidization and fouling propensity and to optimize the reactor configuration to ensure a better handling of the system and a more stable operation.

## REFERENCES

- AHMED, F. N. & LAN, C. Q. 2012. Treatment of landfill leachate using membrane bioreactors: A review. *Desalination*, 287, 41-54.
- AKAMATSU, K., LU, W., SUGAWARA, T. & NAKAO, S.-I. 2010. Development of a novel fouling suppression system in membrane bioreactors using an intermittent electric field. *Water Research*, 44, 825-830.
- ALBERTSEN, M., KARST, S. M., ZIEGLER, A. S., KIRKEGAARD, R. H. & NIELSEN, P. H. 2015. Back to basics—the influence of DNA extraction and primer choice on phylogenetic analysis of activated sludge communities. *PloS one*, 10, e0132783.
- ASLAM, M. & KIM, J. 2019. Investigating membrane fouling associated with GAC fluidization on membrane with effluent from anaerobic fluidized bed bioreactor in domestic wastewater treatment. *Environmental Science and Pollution Research*, 26, 1170-1180.
- ASLAM, M., YANG, P., LEE, P.-H. & KIM, J. 2018. Novel staged anaerobic fluidized bed ceramic membrane bioreactor: Energy reduction, fouling control and microbial characterization. *Journal of Membrane Science*, 553, 200-208.
- BARUA, S., ZAKARIA, B. S., LIN, L. & DHAR, B. R. 2019. Shaping microbial communities with conductive carbon fibers to enhance methane productivity and kinetics. *Bioresource Technology Reports*, 5, 20-27.
- BOLGER, A. M., LOHSE, M. & USADEL, B. 2014. Trimmomatic: a flexible trimmer for Illumina sequence data. *Bioinformatics*, 30, 2114-2120.
- BOREA, L., PUIG, S., MONCLÚS, H., NADDEO, V., COLPRIM, J. & BELGIORNO, V. 2017. Microbial fuel cell technology as a downstream process of a membrane bioreactor for sludge reduction. *Chemical Engineering Journal*, 326, 222-230.
- CAO, Z., LI, S., ZHANG, J. & ZHANG, H. 2017. An electro-microbial membrane system with anti-fouling function for phenol wastewater treatment: An electro-microbial membrane system with anti-fouling. *Journal of Chemical Technology & Biotechnology*, 92, 693-699.
- CAPORASO, J. G., KUCZYNSKI, J., STOMBAUGH, J., BITTINGER, K., BUSHMAN, F. D., COSTELLO, E. K., FIERER, N., PENA, A. G., GOODRICH, J. K. & GORDON, J. I. 2010. QIIME allows analysis of high-throughput community sequencing data. *Nature methods*, 7, 335.
- CHENG, Q. & CALL, D. F. 2016. Hardwiring microbes via direct interspecies electron transfer: mechanisms and applications. *Environmental Science: Processes & Impacts*, 18, 968-980.
- CONRAD, R. 1999. Contribution of hydrogen to methane production and control of hydrogen concentrations in methanogenic soils and sediments. *FEMS Microbiology Ecology*, 28, 193-202.

- CUSICK, R. D., BRYAN, B., PARKER, D. S., MERRILL, M. D., MEHANNA, M., KIELY, P. D., LIU, G. & LOGAN, B. E. 2011. Performance of a pilot-scale continuous flow microbial electrolysis cell fed winery wastewater. *Applied Microbiology and Biotechnology*, 89, 2053-2063.
- DING, A., FAN, Q., CHENG, R., SUN, G., ZHANG, M. & WU, D. 2018. Impacts of applied voltage on microbial electrolysis cell-anaerobic membrane bioreactor (MEC-AnMBR) and its membrane fouling mitigation mechanism. *Chemical Engineering Journal*, 333, 630-635.
- EDGAR, R. C. 2013. UPARSE: highly accurate OTU sequences from microbial amplicon reads. *Nature methods*, 10, 996.
- ENZMANN, F., MAYER, F., ROTHER, M. & HOLTSMANN, D. 2018. Methanogens: biochemical background and biotechnological applications. *AMB Express*, 8, 1.
- FENG, Q., SONG, Y.-C. & AHN, Y. 2018. Electroactive microorganisms in bulk solution contribute significantly to methane production in bioelectrochemical anaerobic reactor. *Bioresource Technology*, 259, 119-127.
- GAJARAJ, S. & HU, Z. 2014. Integration of microbial fuel cell techniques into activated sludge wastewater treatment processes to improve nitrogen removal and reduce sludge production. *Chemosphere*, 117, 151-157.
- GKOTSIS, P. K. & ZOUBOULIS, A. I. 2019. Biomass Characteristics and Their Effect on Membrane Bioreactor Fouling. *Molecules (Basel, Switzerland)*, 24, 2867.
- HASHISHO, J. & EL-FADEL, M. 2016. Membrane bioreactor technology for leachate treatment at solid waste landfills. *Reviews in Environmental Science and Bio/Technology*, 15, 441-463.
- KATURI, K. P., ALI, M. & SAIKALY, P. E. 2019. The role of microbial electrolysis cell in urban wastewater treatment: integration options, challenges, and prospects. *Current Opinion in Biotechnology*, 57, 101-110.
- KATURI, K. P., KALATHIL, S., RAGAB, A. A., BIAN, B., ALQAHTANI, M. F., PANT, D. & SAIKALY, P. E. 2018. Dual-function electrocatalytic and macroporous hollow-fiber cathode for converting waste streams to valuable resources using microbial electrochemical systems. *Advanced Materials*, 30, 1707072.
- KATURI, K. P., KAVANAGH, P., RENGARAJ, S. & LEECH, D. 2010. *Geobacter sulfurreducens* biofilms developed under different growth conditions on glassy carbon electrodes: insights using cyclic voltammetry. *Chemical communications (Cambridge, England)*, 46, 4758.
- KATURI, K. P., WERNER, C. M., JIMENEZ-SANDOVAL, R. J., CHEN, W., JEON, S., LOGAN, B. E., LAI, Z., AMY, G. L. & SAIKALY, P. E. 2014. A novel anaerobic electrochemical membrane bioreactor (AnEMBR) with conductive hollow-fiber membrane for treatment of low-organic strength solutions. *Environmental science & technology*, 48, 12833-12841.

- KHAN, M. A., NGO, H. H., GUO, W. S., LIU, Y. W., ZHOU, J. L., ZHANG, J., LIANG, S., NI, B. J., ZHANG, X. B. & WANG, J. 2016. Comparing the value of bioproducts from different stages of anaerobic membrane bioreactors. *Bioresource Technology*, 214, 816-825.
- KIM, J., KIM, K., YE, H., LEE, E., SHIN, C., MCCARTY, P. L. & BAE, J. 2011. Anaerobic Fluidized Bed Membrane Bioreactor for Wastewater Treatment. *Environmental Science & Technology*, 45, 576-581.
- KRZEMINSKI, P., LEVERETTE, L., MALAMIS, S. & KATSOU, E. 2017. Membrane bioreactors – A review on recent developments in energy reduction, fouling control, novel configurations, LCA and market prospects. *Journal of Membrane Science*, 527, 207-227.
- KUMAR, S. S., MALYAN, S. K., BASU, S. & BISHNOI, N. R. 2017. Syntrophic association and performance of Clostridium, Desulfovibrio, Aeromonas and Tetrathlobacter as anodic biocatalysts for bioelectricity generation in dual chamber microbial fuel cell. *Environmental Science and Pollution Research*, 24, 16019-16030.
- LI, J., GE, Z. & HE, Z. 2014. Advancing membrane bioelectrochemical reactor (MBER) with hollow-fiber membranes installed in the cathode compartment. *Journal of Chemical Technology & Biotechnology*, 89, 1330-1336.
- LIAO, B.-Q., KRAEMER, J. T. & BAGLEY, D. M. 2006. Anaerobic membrane bioreactors: applications and research directions. *Critical Reviews in Environmental Science and Technology*, 36, 489-530.
- LIN, H., PENG, W., ZHANG, M., CHEN, J., HONG, H. & ZHANG, Y. 2013. A review on anaerobic membrane bioreactors: Applications, membrane fouling and future perspectives. *Desalination*, 314, 169-188.
- LIN, R., CHENG, J., ZHANG, J., ZHOU, J., CEN, K. & MURPHY, J. D. 2017. Boosting biomethane yield and production rate with graphene: The potential of direct interspecies electron transfer in anaerobic digestion. *Bioresource Technology*, 239, 345-352.
- LIU, F., ROTARU, A.-E., SHRESTHA, P. M., MALVANKAR, N. S., NEVIN, K. P. & LOVLEY, D. R. 2012. Promoting direct interspecies electron transfer with activated carbon. *Energy & Environmental Science*, 5, 8982-8989.
- LIU, H., HU, H., CHIGNELL, J. & FAN, Y. 2010. Microbial electrolysis: novel technology for hydrogen production from biomass. *Biofuels*, 1, 129-142.
- LIU, J., LIU, L., GAO, B. & YANG, F. 2013. Integration of bio-electrochemical cell in membrane bioreactor for membrane cathode fouling reduction through electricity generation. *Journal of Membrane Science*, 430, 196-202.
- LIU, J., LIU, L., GAO, B., YANG, F., CRITTENDEN, J. & REN, N. 2014. Integration of microbial fuel cell with independent membrane cathode bioreactor for power generation, membrane fouling mitigation and wastewater treatment. *International Journal of Hydrogen Energy*, 39, 17865-17872.
- LOGAN, B. & RABAEY, K. 2012. Conversion of Wastes into Bioelectricity and Chemicals by Using Microbial Electrochemical Technologies. *Science (New York, N.Y.)*, 337, 686-90.

- LOHNER, S. T., DEUTZMANN, J. S., LOGAN, B. E., LEIGH, J. & SPORMANN, A. M. 2014. Hydrogenase-independent uptake and metabolism of electrons by the archaeon *Methanococcus maripaludis*. *The ISME Journal*, 8, 1673-1681.
- LOVLEY, D. R. 2012. Electromicrobiology. *Annual Review of Microbiology*, 66, 391-409.
- LOVLEY, D. R., UEKI, T., ZHANG, T., MALVANKAR, N. S., SHRESTHA, P. M., FLANAGAN, K. A., AKLUJKAR, M., BUTLER, J. E., GILOTEAUX, L., ROTARU, A.-E., HOLMES, D. E., FRANKS, A. E., ORELLANA, R., RISSO, C. & NEVIN, K. P. 2011. *Geobacter*: The Microbe Electric's Physiology, Ecology, and Practical Applications. In: POOLE, R. K. (ed.) *Advances in Microbial Physiology*. Academic Press.
- LUO, J., QIAN, G., LIU, J. & XU, Z. P. 2015. Anaerobic methanogenesis of fresh leachate from municipal solid waste: A brief review on current progress. *Renewable and Sustainable Energy Reviews*, 49, 21-28.
- MA, J., WANG, Z., ZOU, X., FENG, J. & WU, Z. 2013. Microbial communities in an anaerobic dynamic membrane bioreactor (AnDMBR) for municipal wastewater treatment: Comparison of bulk sludge and cake layer. *Process Biochemistry*, 48, 510-516.
- MALAEB, L., KATURI, K. P., LOGAN, B. E., MAAB, H., NUNES, S. P. & SAIKALY, P. E. 2013. A hybrid microbial fuel cell membrane bioreactor with a conductive ultrafiltration membrane biocathode for wastewater treatment. *Environmental science & technology*, 47, 11821-11828.
- MELIN, T., JEFFERSON, B., BIXIO, D., THOEYE, C., DE WILDE, W., DE KONING, J., VAN DER GRAAF, J. & WINTGENS, T. 2006. Membrane bioreactor technology for wastewater treatment and reuse. *Desalination*, 187, 271-282.
- PARK, J.-H., KANG, H.-J., PARK, K.-H. & PARK, H.-D. 2018a. Direct interspecies electron transfer via conductive materials: A perspective for anaerobic digestion applications. *Bioresource Technology*, 254, 300-311.
- PARK, J.-H., PARK, J.-H., JE SEONG, H., SUL, W. J., JIN, K.-H. & PARK, H.-D. 2018b. Metagenomic insight into methanogenic reactors promoting direct interspecies electron transfer via granular activated carbon. *Bioresource Technology*, 259, 414-422.
- PECHAN, P., DE VRIES, G. E. & SPRINGERLINK 2013. *Living with Water: Targeting Quality in a Dynamic World*, New York, NY, Springer New York.
- QUAIST, C., PRUESSE, E., YILMAZ, P., GERKEN, J., SCHWEER, T., YARZA, P., PEPLIES, J. & GLÖCKNER, F. O. 2012. The SILVA ribosomal RNA gene database project: improved data processing and web-based tools. *Nucleic acids research*, 41, D590-D596.
- R BOND, D., HOLMES, D., M TENDER, L. & R LOVLEY, D. 2002. Bond DR, Holmes DE, Tender LM, Lovley DR.. Electrode-reducing microorganisms that harvest energy from marine sediments. *Science* 295: 483-485. *Science (New York, N.Y.)*, 295, 483-5.
- R LOVLEY, D. 2006. Bug Juice: Harvesting Electricity with Microorganisms. *Nature reviews. Microbiology*, 4, 497-508.
- R. LOVLEY, D. 2017. Syntrophy Goes Electric: Direct Interspecies Electron Transfer. *Annual Review of Microbiology*, 71.

- REGUERA, G., MCCARTHY, K. D., MEHTA, T., NICOLL, J. S., TUOMINEN, M. T. & LOVLEY, D. R. 2005. Extracellular electron transfer via microbial nanowires. *Nature*, 435, 1098-1101.
- REIMERS, C., LI, C., F. GRAW, M., SCHRADER, P. & WOLF, M. 2017. The Identification of Cable Bacteria Attached to the Anode of a Benthic Microbial Fuel Cell: Evidence of Long Distance Extracellular Electron Transport to Electrodes. *Frontiers in Microbiology*, 8.
- REN, L., AHN, Y. & LOGAN, B. E. 2014. A Two-Stage Microbial Fuel Cell and Anaerobic Fluidized Bed Membrane Bioreactor (MFC-AFMBR) System for Effective Domestic Wastewater Treatment. *Environmental Science & Technology*, 48, 4199-4206.
- ROTARU, A.-E., SHRESTHA, P., LIU, F., SHRESTHA, M., SHRESTHA, D., EMBREE, M., ZENGLER, K., WARDMAN, C., P. NEVIN, K. & R. LOVLEY, D. 2014a. A new model for electron flow during anaerobic digestion: direct interspecies electron transfer to *Methanosaeta* for the reduction of carbon dioxide to methane. *Energy & Environmental Science*, 7, 408-415.
- ROTARU, A.-E., SHRESTHA, P. M., LIU, F., MARKOVAITE, B., CHEN, S., NEVIN, K. P. & LOVLEY, D. R. 2014b. Direct Interspecies Electron Transfer between *Geobacter metallireducens* and *Methanosarcina barkeri*. *Applied and Environmental Microbiology*, 80, 4599.
- ROTARU, A.-E., SHRESTHA, P. M., LIU, F., MARKOVAITE, B., CHEN, S., NEVIN, K. P. & LOVLEY, D. R. 2014c. Direct interspecies electron transfer between *Geobacter metallireducens* and *Methanosarcina barkeri*. *Applied and environmental microbiology*, 80, 4599-4605.
- SAPIREDDY, V., RAGAB, A. A., KATURI, K. P., YU, Y., LAI, Z., LI, E., THORODDSEN, S. T. & SAIKALY, P. E. 2019. Effect of specific cathode surface area on biofouling in an anaerobic electrochemical membrane bioreactor: Novel insights using high-speed video camera. *Journal of Membrane Science*, 577, 176-183.
- SHIN, C. & BAE, J. 2018. Current status of the pilot-scale anaerobic membrane bioreactor treatments of domestic wastewaters: A critical review. *Bioresource Technology*, 247, 1038-1046.
- SIEBER, J. R., MCINERNEY, M. J. & GUNSALUS, R. P. 2012. Genomic Insights into Syntrophy: The Paradigm for Anaerobic Metabolic Cooperation. *Annual Review of Microbiology*, 66, 429-452.
- SU, X., TIAN, Y., SUN, Z., LU, Y. & LI, Z. 2013. Performance of a combined system of microbial fuel cell and membrane bioreactor: wastewater treatment, sludge reduction, energy recovery and membrane fouling. *Biosensors & bioelectronics* 49, 92.
- SUTHERLAND, K. 2010. The rise of membrane bioreactors. *Filtration & Separation*, 47, 14-16.

- TCHOBANOGLIOUS, G., BURTON, F. L., STENSEL, H. D., METCALF & EDDY 2003. *Wastewater engineering: treatment and reuse*, Boston, McGraw Hill.
- THAUER, R. K., KASTER, A.-K., SEEDORF, H., BUCKEL, W. & HEDDERICH, R. 2008. Methanogenic archaea: ecologically relevant differences in energy conservation. *Nature Reviews Microbiology*, 6, 579-591.
- TIAN, Y., JI, C., WANG, K. & LE-CLECH, P. 2014. Assessment of an anaerobic membrane bio-electrochemical reactor (AnMBER) for wastewater treatment and energy recovery. *Journal of Membrane Science*, 450, 242-248.
- TIAN, Y., LI, H., LI, L., SU, X., LU, Y., ZUO, W. & ZHANG, J. 2015. In-situ integration of microbial fuel cell with hollow-fiber membrane bioreactor for wastewater treatment and membrane fouling mitigation. *Biosensors and Bioelectronics*, 64, 189-195.
- TRZCINSKI, A. P. & STUCKEY, D. C. 2016. Effect of sparging rate on permeate quality in a submerged anaerobic membrane bioreactor (SAMBR) treating leachate from the organic fraction of municipal solid waste (OFMSW). *Journal of Environmental Management*, 168, 67-73.
- WANG, J., BI, F., NGO, H.-H., GUO, W., JIA, H., ZHANG, H. & ZHANG, X. 2016. Evaluation of energy-distribution of a hybrid microbial fuel cell-membrane bioreactor (MFC-MBR) for cost-effective wastewater treatment. *Bioresource technology* 200, 420.
- WANG, Y.-K., SHENG, G.-P., LI, W.-W., HUANG, Y.-X., YU, Y.-Y., ZENG, R. J. & YU, H.-Q. 2011. Development of a Novel Bioelectrochemical Membrane Reactor for Wastewater Treatment. *Environmental Science & Technology*, 45, 9256-9261.
- WANG, Y.-K., SHENG, G.-P., SHI, B.-J., LI, W.-W. & YU, H.-Q. 2013. *A Novel Electrochemical Membrane Bioreactor as a Potential Net Energy Producer for Sustainable Wastewater Treatment*.
- WANG, Y.-P., LIU, X.-W., LI, W.-W., LI, F., WANG, Y.-K., SHENG, G.-P., ZENG, R. J. & YU, H.-Q. 2012. A microbial fuel cell–membrane bioreactor integrated system for cost-effective wastewater treatment. *Applied Energy*, 98, 230-235.
- WANG, Y., ZHANG, H., LI, B. & FENG, Y. 2018. Integrating sludge microbial fuel cell with inclined plate settling and membrane filtration for electricity generation, efficient sludge reduction and high wastewater quality. *Chemical Engineering Journal*, 331, 152-160.
- WERNER, C. M., KATURI, K. P., HARI, A. R., CHEN, W., LAI, Z., LOGAN, B. E., AMY, G. L. & SAIKALY, P. E. 2016. Graphene-Coated Hollow Fiber Membrane as the Cathode in Anaerobic Electrochemical Membrane Bioreactors – Effect of Configuration and Applied Voltage on Performance and Membrane Fouling. *Environmental Science & Technology*, 50, 4439-4447.
- XU, L., ZHANG, G.-Q., YUAN, G.-E., LIU, H.-Y., LIU, J.-D. & YANG, F.-L. 2015. Anti-fouling performance and mechanism of anthraquinone/polypyrrole composite modified membrane cathode in a novel MFC-aerobic MBR coupled system. *RSC Advances*, 5, 22533-22543.



- YEE, M. O. & ROTARU, A.-E. 2020. Extracellular electron uptake in Methanosarcinales is independent of multiheme c-type cytochromes. *Scientific Reports*, 10, 372.
- YIN, Q., ZHU, X., ZHAN, G., BO, T., YANG, Y., TAO, Y., HE, X., LI, D. & YAN, Z. 2016. Enhanced methane production in an anaerobic digestion and microbial electrolysis cell coupled system with co-cultivation of *Geobacter* and *Methanosarcina*. *Journal of environmental sciences (China)*, 42, 210-214.
- YOO, R., KIM, J., MCCARTY, P. L. & BAE, J. 2012. Anaerobic treatment of municipal wastewater with a staged anaerobic fluidized membrane bioreactor (SAF-MBR) system. *Bioresource Technology*, 120, 133-139.
- ZHAO, Z., ZHANG, Y., WANG, L.-Y. & QUAN, X. 2015. Potential for direct interspecies electron transfer in an electric-anaerobic system to increase methane production from sludge digestion. *Scientific Reports*, 5, 11094.

## APPENDIX A

Table 4: Acetate and COD removal data

Time (Weeks of Operation)	AnFMBR-MEC1		AnFMBR-MEC2	
	COD	Acetate	COD	Acetate
1	99.46428571	-	99.46428571	-
2	11.60714286	-	13.80952381	-
3	23.21428571	95.4181856	43.57142857	94.272732
4	37.5	76.23619388	57.85714286	71.47669682
5	72.38095238	75.33833057	60.57142857	75.23551304
6	64.76190476	73.11051123	63.21428571	79.15491064
7	70.35714286	76.15709421	65.35714286	86.89906797
8	56.53061224	80.18664309	57.85714286	92.24113399
9	85	80.238312	60.45918367	89.94441215
10	57.5	87.09877091	79.52380952	90.9836801
11	86.50793651	74.95264006	80.47619048	-
12	85.71428571	95.4181856	77.14285714	89.92541945
13	83.33333333	95.4181856	87.14285714	94.272732
14	94.10714286	95.4181856	90.95238095	94.272732
15	88.03571429	95.4181856	93.80952381	94.272732
16	87.5	95.4181856	87.85714286	94.272732
17	95	95.4181856	92.5	94.272732
18	97.85714286	95.4181856	96.42857143	94.272732
19	92.5	95.4181856	93.57142857	94.272732
20	94.10714286	95.4181856	87.5	95.39266172
21	94.46428571	95.4181856	93.03571429	94.272732
22	95.53571429	95.4181856	95.53571429	94.272732
23	92.14285714	95.4181856	93.57142857	94.272732
24	95.89285714	95.4181856	95.53571429	94.272732
25	94.28571429	95.4181856	96.60714286	94.272732
26	93.39285714	95.4181856	96.42857143	94.272732
27	95.53571429	95.4181856	95.53571429	94.272732

Table 5: Energy parameters during operation

Weeks of Operation	AnFMBR-MEC2												
	Voltage (V)	Current (A)	Coulomb (C)	CE (%)	n <sub>CE</sub> (moles)	I <sub>v</sub> (A/m <sup>3</sup> )	Q <sub>th</sub> (m <sup>3</sup> /m <sup>3</sup> /d)	W <sub>E</sub> (kwh/m <sup>3</sup> )	CH <sub>4</sub> (mL/d)	Q <sub>CH<sub>4</sub></sub> (m <sup>3</sup> /m <sup>3</sup> /d)	n <sub>CH<sub>4</sub></sub> (moles)	W <sub>CH<sub>4</sub></sub> (kWh/m <sup>3</sup> )	Γ <sub>cat</sub>
1	235.66	0.0236	2033.02	29.03	0.0079	15.71	0.0426	0.1703	190.34	0.0634	0.0079	0.65	177.71
2	372.62	0.0373	3219.81	45.97	0.0292	24.84	0.0673	0.1951	166.61	0.0159	0.0069	0.16	23.31
3	407.11	0.0407	3515.79	50.20	0.0319	27.14	0.0736	0.1898	0.43	0.0000	0.0000	0.00	0.06
4	393.65	0.0394	3447.69	49.23	0.0313	26.24	0.0711	0.1920	31.97	0.0030	0.0013	0.03	4.08
5	410.24	0.0410	3544.87	50.61	0.0321	27.35	0.0741	0.1901	10.12	0.0010	0.0004	0.01	1.30
6	395.21	0.0395	3415.87	48.77	0.0310	26.35	0.0714	0.1924	37.37	0.0036	0.0015	0.04	5.13
7	358.99	0.0359	3101.41	44.28	0.0281	23.93	0.0649	0.1957	111.02	0.0106	0.0046	0.11	16.41
8	344.50	0.0344	2957.98	42.23	0.0268	22.97	0.0623	0.1957	151.82	0.0145	0.0063	0.15	23.50
9	319.89	0.0320	2770.84	39.56	0.0251	21.33	0.0578	0.1933	277.19	0.0264	0.0114	0.27	47.00
10	209.82	0.0210	1812.86	25.88	0.0164	13.99	0.0379	0.1640	416.71	0.0397	0.0172	0.41	103.92
11	173.59	0.0174	1499.81	21.41	0.0136	11.57	0.0314	0.1453	241.39	0.0230	0.0100	0.23	77.86
12	204.16	0.0204	1763.94	25.19	0.0160	13.61	0.0369	0.1607	105.57	0.0101	0.0044	0.10	27.47
13	195.46	0.0195	1688.80	24.11	0.0153	13.03	0.0353	0.1566	326.55	0.0311	0.0135	0.32	91.35
14	182.71	0.0183	1578.62	22.54	0.0143	12.18	0.0330	0.1506	232.01	0.0221	0.0096	0.23	68.70
15	183.53	0.0184	1585.66	22.64	0.0144	12.24	0.0332	0.1506	328.06	0.0312	0.0135	0.32	93.68
16	184.66	0.0185	1595.48	22.78	0.0145	12.31	0.0334	0.1512	372.29	0.0355	0.0154	0.36	104.62
17	251.47	0.0251	2172.72	31.02	0.0197	16.76	0.0455	0.1791	497.40	0.0474	0.0205	0.48	106.37
18	263.26	0.0263	2276.35	32.50	0.0206	17.55	0.0476	0.1836	274.47	0.0261	0.0113	0.27	54.16
19	142.58	0.0143	1248.76	17.83	0.0113	9.51	0.0258	0.1222	320.26	0.0305	0.0132	0.31	131.79
20	127.21	0.0127	1100.89	15.72	0.0100	8.48	0.0230	0.1147	373.09	0.0355	0.0154	0.36	180.02
21	300.55	0.0301	2597.72	37.09	0.0236	20.04	0.0543	0.1919	264.41	0.0252	0.0109	0.26	46.26
22	197.07	0.0197	1709.04	24.40	0.0155	13.14	0.0356	0.1468	450.77	0.0429	0.0186	0.44	150.66
23	191.99	0.0192	1658.57	23.68	0.0150	12.80	0.0347	0.1553	275.09	0.0262	0.0114	0.27	77.33
24	239.29	0.0239	2066.30	29.50	0.0187	15.95	0.0432	0.1754	398.22	0.0379	0.0164	0.39	88.33
25	221.60	0.0222	1916.32	27.36	0.0174	14.77	0.0401	0.1688	269.87	0.0257	0.0111	0.26	67.52
26	186.76	0.0187	1672.67	23.88	0.0152	12.45	0.0338	0.1531	314.12	0.0299	0.0130	0.31	86.24
27	189.36	0.0189	1640.08	23.42	0.0085	12.62	0.0342	0.1547	266.52	0.0444	0.0110	0.45	129.57

## **Archaeal and bacterial community analysis targeting 16S V4 rRNA**

### **Library preparation**

Archaea and Bacteria, 16S rRNA gene region V4 sequencing libraries were prepared by a custom protocol based on an Illumina protocol (Illumina, 2015). Up to 10 ng of extracted DNA was used as template for PCR amplification of the Archaea and Bacteria, 16S rRNA gene region V4 amplicons. Each PCR reaction (25  $\mu$ L) contained (12.5  $\mu$ L) PCR BIO Ultra mix (PCR Biosystems, USA) and 400 nM of each forward and reverse tailed primer mix. PCR was conducted with the following program: Initial denaturation at 95  $^{\circ}$ C for 2 min, 30 cycles of amplification (95  $^{\circ}$ C for 15 s, 55  $^{\circ}$ C for 15 s, 72  $^{\circ}$ C for 50 s) and a final elongation at 72  $^{\circ}$ C for 5 min. Duplicate PCR reactions were performed for each sample and the duplicates were pooled after PCR. The forward and reverse tailed primers were designed according to (Illumina, 2015) and contain primers targeting the Archaea and Bacteria, 16S rRNA gene region V4: [515F] GTGYCAGCMGCCGCGGTA and [805R] GACTACHVGGGTATCTAATCC (Ye et al., 2016). The primer tails enable attachment of Illumina Nextera adaptors necessary for sequencing in a subsequent PCR. The resulting amplicon libraries were purified using the standard protocol for Agencourt Ampure XP Beads (Beckman Coulter, USA) with a bead to sample ratio of 4:5. DNA was eluted in 25  $\mu$ L of nuclease free water (Qiagen, Germany). DNA concentration was measured using Qubit dsDNA HS Assay kit (Thermo Fisher Scientific, USA). Gel electrophoresis using TapeStation 2200 and D1000/High sensitivity D1000 screentapes (Agilent, USA) was used to validate product size and purity of a subset of sequencing libraries. Sequencing libraries were prepared from the purified amplicon libraries using a second PCR. Each PCR reaction (25  $\mu$ L) contained PCR BIO HiFi buffer (1x), PCR BIO HiFi Polymerase (1 U/reaction) (PCRBiosystems, UK), adaptor mix (400 nM of each forward and reverse) and up to 10 ng of amplicon library template. PCR was conducted with the following program: Initial

denaturation at 95 °C for 2 min, 8 cycles of amplification (95 °C for 20 s, 55 °C for 30 s, 72 °C for 60 s) and a final elongation at 72 °C for 5 min. The resulting sequencing libraries were purified using the standard protocol for Agencourt Ampure XP Beads (Beckman Coulter, USA) with a bead to sample ratio of 4:5. DNA was eluted in 25 µL of nuclease free water (Qiagen, Germany). DNA concentration was measured using Qubit dsDNA HS Assay kit (Thermo Fisher Scientific, USA). Gel electrophoresis using TapeStation 2200 and D1000/High sensitivity D1000 screentapes (Agilent, USA) was used to validate product size and purity of a subset of sequencing libraries.

### **DNA sequencing**

The purified sequencing libraries were pooled in equimolar concentrations and diluted to 2 nM. The samples were paired-end sequenced (2x300 bp) on a MiSeq (Illumina, USA) using a MiSeq Reagent kit v3 (Illumina, USA) following the standard guidelines for preparing and loading samples on the MiSeq. >10% PhiX control library was spiked in to overcome low complexity issues often observed with amplicon samples.

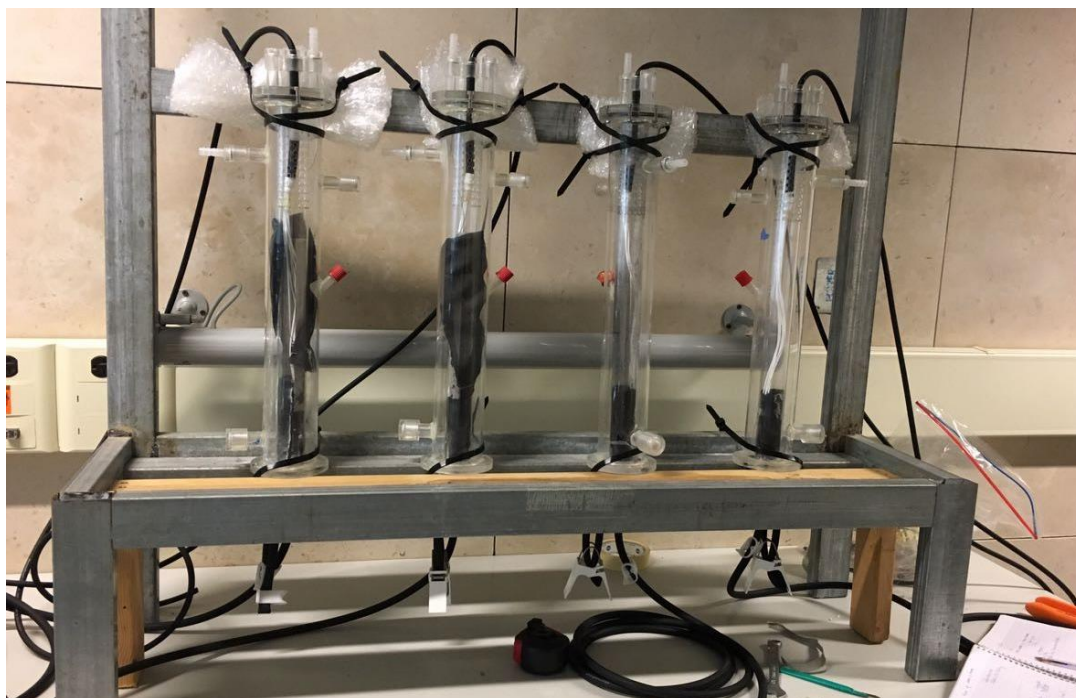


Figure 9: Experimental set-up during installation

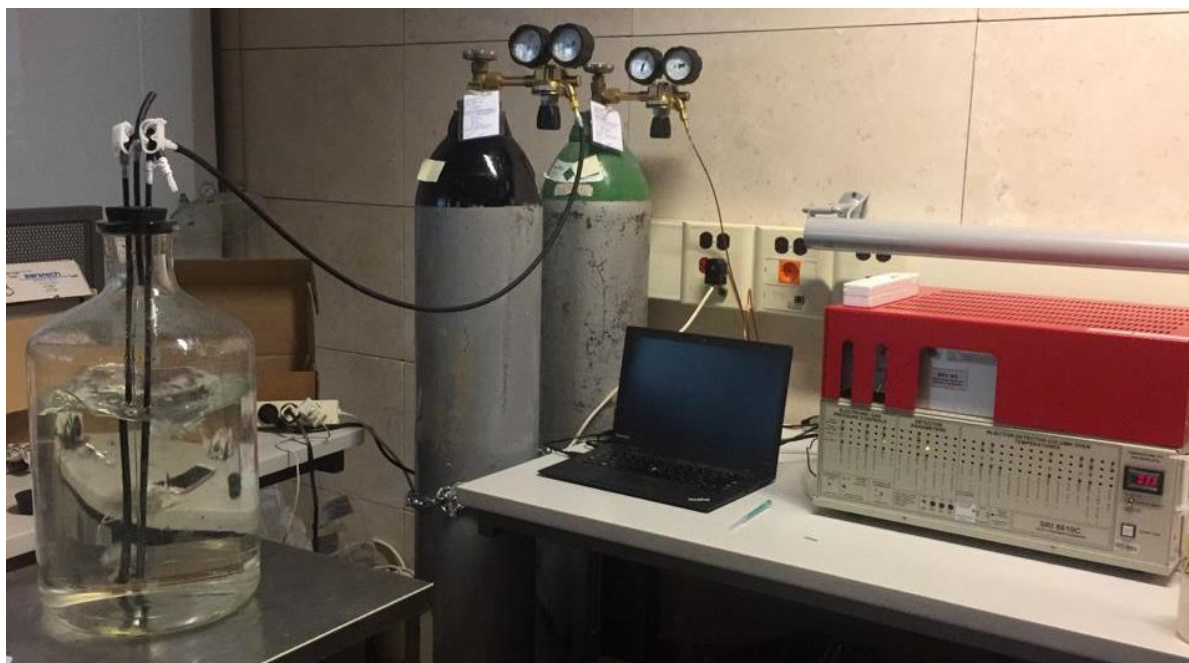


Figure 10: Purging the synthetic feed tank with nitrogen (GC Unit on the right)

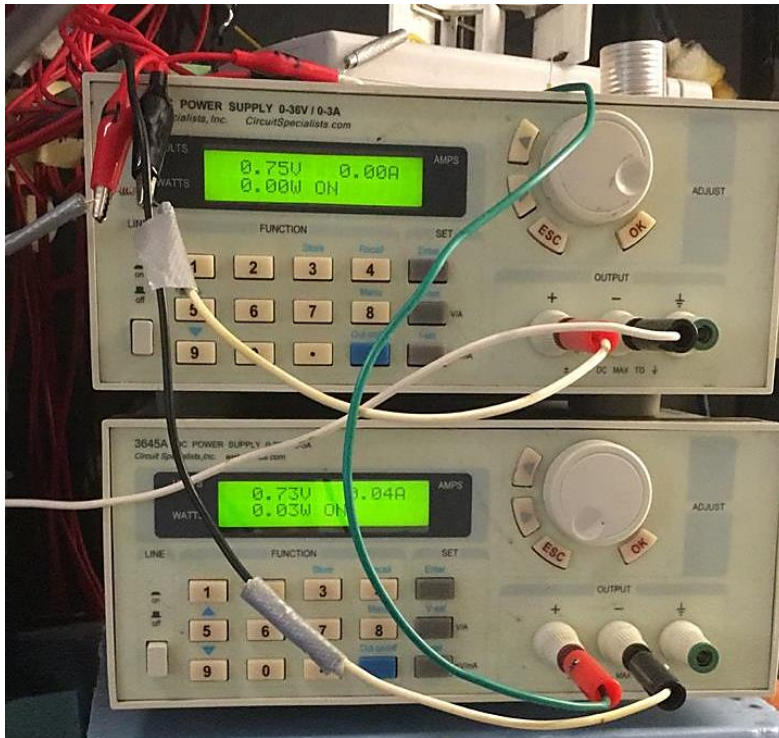


Figure 11: Power supply unit



Figure 12: Experimental set-up during operation